

# Asymptotically perfect seeded graph matching without edge correlation (and applications to inference)

Tong Qi<sup>1</sup>, Vera Andersson<sup>1</sup>, Peter Viechnicki<sup>2</sup>, and Vince Lyzinski<sup>1</sup>

<sup>1</sup>Department of Mathematics, University of Maryland, College Park

<sup>2</sup>Human Language Technology Center of Excellence, Johns Hopkins University

July 4, 2025

## Abstract

We present the **OmniMatch** algorithm for seeded multiple graph matching. In the setting of  $d$ -dimensional Random Dot Product Graphs (RDPG), we prove that under mild assumptions, **OmniMatch** with  $s$  seeds asymptotically and efficiently perfectly aligns  $O(s^\alpha)$  unseeded vertices—for  $\alpha < 2 \wedge d/4$ —across multiple networks even in the presence of no edge correlation. We demonstrate the effectiveness of our algorithm across numerous simulations and in the context of shuffled graph hypothesis testing. In the shuffled testing setting, testing power is lost due to the misalignment/shuffling of vertices across graphs, and we demonstrate the capacity of **OmniMatch** to correct for misaligned vertices prior to testing and hence recover the lost testing power. We further demonstrate the algorithm on a pair of data examples from connectomics and machine translation.

## 1 Introduction and Background

Graphs and network data structures are fundamental tools for modeling complex systems of interacting objects across disciplines including biology, neuroscience [49, 19, 52], and social sciences [26, 42]. For instance, in neuroscience connectomics [54] regions of interest (ROIs) in the brain can be represented as nodes, while the functional connectivity between these regions can be modeled via the edge structure of the graphs. In the context of social networks [67], individuals are represented as nodes, and social relationships or interactions between individuals are denoted by edges. In the context of natural language processing, words or concepts can be represented as nodes [40], and those documents containing those nodes can be further represented as graphs where nodes are adjacent based on some properties of the documents. These graph representations provide a versatile framework for analyzing the structural and relational properties of complex systems. Comparing and analyzing graphs is essential for numerous tasks, including understanding structural patterns, detecting anomalies, and hypothesis testing between two graph samples. However, a persistent challenge in graph comparison arises when node correspondences are unknown or partially scrambled

[64, 56], as often encountered in applications such as brain connectomics [63], anonymized social networks, or language processing [40].

Traditional multiple graph inference methodologies such as two-sample testing [58, 16, 5], tensor decomposition [72, 73, 2], multiple graph community detection [28, 48, 44], etc., typically rely on the assumption that node identities are perfectly aligned and observed across graphs. When this is not the case inferential performance can degrade [56, 64, 35], although graph matching methods [13, 69, 17] can be applied to align the networks, recover the missing cross-graph node labels, and recover inferential performance. Despite these recent advancements, statistical inference under node misalignment remains underdeveloped. When a subset of nodes is shuffled or unaligned between graphs, recovering the correct node correspondences becomes essential to accurately reconstruct the underlying graph structure and enable valid comparisons.

There is a robust graph matching literature both from the algorithmic and theoretic perspectives (see Section 3.1 for further background on graph matching), though most existing theoretical work (both information theoretic bounds on de-anonymization and theoretical algorithmic guarantees) relies on the presence of edge correlation across graphs to anchor the alignment. In this paper, we address the problem of *seeded* multiple graph matching in the setting where there is no edge correlation. Seeds here refer to vertices across the multiple graphs whose correspondence is known *a priori* [41, 20, 38]; multiple graph matching refers to the problem of simultaneously aligning the vertices across multiple networks. To tackle this problem, we propose the **OmnMatch** algorithm which jointly embeds the seeded vertices across a collection of graphs, out-of-sample embeds the unseeded vertices, and then aligns unseeded nodes by solving an approximate defined linear assignment problem in the embedded space. This integrated approach allows us to leverage expertise in graph embeddings [6] (see Section 1.1) to efficiently, provably asymptotically perfectly match uncorrelated graphs in the general Random Dot Product Graph setting (under mild model assumptions). To our knowledge, this is the first result proving asymptotically perfect matching in this RDPG model (in either theory or algorithmically) in the absence of edge correlation. **OmnMatch** is then further used to perform robust statistical inference by combining node matching with hypothesis testing, enabling valid comparisons even in the presence of node shuffling.

This paper is organized as follows. We describe the Random Dot Product Graph model and joint graph embedding framework in Section 1.1, the graph alignment and matching problem in Section 1.2, and graph hypothesis testing more thoroughly Sections 1.3. We introduce the new algorithm **OmnMatch** in Section 2 with our main theoretical results on its graph matching performance with multiple seeds. In Section 3, we show our simulation results on both graph matching and hypothesis testing with **OmnMatch** and results using real brain data. We discuss this new algorithm in Section 4.

**Notation:** The following notation will be used throughout. For positive integer  $n$ , we write  $[n]$  to denote  $[n] = \{1, 2, 3, \dots, n\}$  and we write  $\vec{1}_n$  to denote the  $n$ -dimensional vector of all 1's. We write  $\|\cdot\|$  as the Euclidean norm on vectors and the spectral norm on matrices,  $\|\cdot\|_F$  as the Frobenius norm,  $\|\cdot\|_{2 \rightarrow \infty}$  as the two-to-infinity norms. The set of  $d \times d$  real orthogonal matrices is denoted by  $\mathcal{O}_d$ . We have  $\mathbf{I}_k$  to denote the  $k \times k$  identity matrix.

## 1.1 Random Graph Models and Joint Graph Embeddings

Our analysis will be couched within the context of Random Dot Product Graphs (RDPG) [70], a class of latent position graph models [27] that are particularly amenable to subsequent analysis [6]. Note that we suspect that all results contained herein can be proven for the more general Generalized RDPG of [55], though the RDPG is suitable for our present purposes.

**Definition 1.1** (Joint Random Dot Product Graph). *Let  $F$  be a distribution on a set  $\mathcal{X} \in \mathbb{R}^d$  satisfying  $\langle x, x' \rangle \in [0, 1]$  for all  $x, x' \in \mathcal{X}$ . Let  $X_1, X_2, \dots, X_n \stackrel{i.i.d.}{\sim} F$ , and let  $P = \mathbf{X}\mathbf{X}^T$ , where  $\mathbf{X} = [X_1^T | X_2^T | \dots | X_n^T]^T \in \mathbb{R}^{n \times d}$ . We say that the random graphs  $(\mathbf{A}^{(1)}, \mathbf{A}^{(2)}, \dots, \mathbf{A}^{(m)})$  are an instantiation of a Joint Random Dot Product Graph model (abbreviated JRDPG), written*

$$(\mathbf{A}^{(1)}, \mathbf{A}^{(2)}, \dots, \mathbf{A}^{(m)}, \mathbf{X}) \sim \text{JRDPG}(F, n, m)$$

if the following holds:

- i. Marginally each  $(\mathbf{A}^{(k)}, \mathbf{X}) \sim \text{RDPG}(F, n)$ ; to wit,  $\mathbf{A}^{(k)}$  is a symmetric, hollow adjacency matrix with above diagonal entries distributed via

$$\mathbb{P}(\mathbf{A}^{(k)} | \mathbf{X}) = \prod_{i < j} (X_i^T X_j)^{A_{ij}^{(k)}} (1 - X_i^T X_j)^{1 - A_{ij}^{(k)}}; \quad (1)$$

Succinctly, conditioned on  $\mathbf{X}$  the above diagonal entries of  $\mathbf{A}^{(k)}$  are independent Bernoulli random variables with success probabilities provided by the corresponding above diagonal entries in  $P$ .

- ii. Conditioned on  $\mathbf{X}$ , the  $\mathbf{A}^{(k)}$ 's are independent

Note that the assumption of independence of the  $\mathbf{A}^{(k)}$ 's in Definition 1.1 is adopted here to emphasize the lack of edge correlation across the graphs we will be aligning with `OmniMatch`. Adding edge correlation across the  $\mathbf{A}^{(k)}$  so as to be suitable for much existing matching theory (e.g., [68, 14, 15, 35]) is easily achieved, see [47] for detail.

One of the key inference tasks in the RDPG framework is estimating the latent position matrix  $\mathbf{X}$ . To this end, spectral methods (in particular the Adjacency Spectral Embedding of [57]) have proven particularly useful. Spectral methods provide suitable estimates  $\hat{\mathbf{X}}$  of  $\mathbf{X}$  that are then amenable to subsequent (more) classical inference methods such as clustering [57, 37, 53], testing [59, 58, 16], classification [60], etc; for a survey of work done in this area, see [6]. The Adjacency Spectral Embedding is defined as follows.

**Definition 1.2** (Adjacency Spectral Embedding (ASE)). *Let  $d \geq 1$  be a positive integer. The  $d$ -dimensional Adjacency Spectral Embedding of a graph  $\mathbf{A}$  into  $\mathbb{R}^d$ , denoted by  $\text{ASE}(\mathbf{A}, d)$ , is defined to be  $\hat{\mathbf{X}} = U_A S_A^{1/2}$ , where*

$$|\mathbf{A}| = (\mathbf{A}^\top \mathbf{A})^{1/2} = \begin{bmatrix} U_A & \tilde{U}_A \end{bmatrix} \begin{bmatrix} S_A & \tilde{S}_A \end{bmatrix} \begin{bmatrix} U_A & \tilde{U}_A \end{bmatrix}^\top,$$

is the spectral decomposition of  $|\mathbf{A}|$ ,  $S_A \in \mathbb{R}^{d \times d}$  is the diagonal matrix with the  $d$  largest eigenvalues of  $|\mathbf{A}|$ , and  $U_A \in \mathbb{R}^{n \times d}$  the corresponding matrix of the  $d$ -largest eigenvectors.

One issue when estimating the latent positions  $\mathbf{X}$  in the RDPG model is the inherent rotational non-identifiability associated with the model [1]: If  $\mathbf{Y} = \mathbf{X}\mathbf{W}$  for a rotation matrix  $\mathbf{W} \in \mathbb{R}^{d \times d}$ , then  $\mathbb{P}(\mathbf{A}|\mathbf{X}) = \mathbb{P}(\mathbf{A}|\mathbf{Y})$ . As such, it is only possible to recover  $\mathbf{X}$  up to a rotation. For single graph inference, this amounts to a requirement the inference task be rotationally invariant. For joint graph inference that rely on graph embeddings, this can be problematic. If the embeddings are done separately, then an additional step (e.g., Procrustes rotation) must be taken to align the graphs in embedding space. The alternative is to construct a joint embedding that simultaneously constructs an aligned embedding for each graph (see, e.g., [32, 4, 66, 76, 72]). Note that the trade-off for not bypassing the need to align is that additional correlation across graphs is often induced in the embedding space by the joint embedding procedure [47].

In the sequel, we will be making use of the *Omnibus Joint Embedding Procedure* (OMNI) of [32]. In OMNI, we are given a collection of  $n$ -vertex graph  $(\mathbf{A}^{(k)})_{k=1}^m$ , the block matrix  $\mathbf{M} \in \mathbb{R}^{mn \times mn}$  is constructed, where the  $i, j$ -th block of  $\mathbf{M}$  is given by  $(\mathbf{A}^{(i)} + \mathbf{A}^{(j)})/2$ . The OMNI embedding of  $(\mathbf{A}^{(k)})_{k=1}^m$  into  $\mathbb{R}^d$  is then given by

$$\hat{\mathbf{X}}_M = \text{OMNI}(\mathbf{A}^{(1)}, \mathbf{A}^{(2)}, \dots, \mathbf{A}^{(m)}) = \text{ASE}(\mathbf{M}, d).$$

In the JRDPG setting outlined above, the OMNI embedding provides a jointly consistent estimator of the true latent position matrix  $\mathbf{X}$ . To wit, we have

**Lemma 1.1** (Lemma 1 in [32]). *Let  $F$  be a distribution on a set  $\mathcal{X} \in \mathbb{R}^d$  satisfying  $\langle x, x' \rangle \in [0, 1]$  for all  $x, x' \in \mathcal{X}$ . Let  $(\mathbf{A}^{(1)}, \mathbf{A}^{(2)}, \dots, \mathbf{A}^{(m)}, \mathbf{X}) \sim \text{JRDPG}(F, n, m)$ , and assume that if  $\mathbf{Y} \sim F$ , then  $\mathbb{E}(\mathbf{Y}\mathbf{Y}^T)$  is rank  $d$ . We have that there exists a constants  $C, C' > 0$  and integer  $\mathfrak{n}$  (depending only on  $F$  and  $m$ ) and an orthogonal matrix  $\mathbf{W}$  such that for  $n \geq \mathfrak{n}$ ,*

$$\|\hat{\mathbf{X}}_M - (\vec{\mathbf{I}}_m \otimes \mathbf{X})\mathbf{W}\|_{2 \rightarrow \infty} \leq \frac{Cm^{1/2} \log(mn)}{\sqrt{n}} \quad (2)$$

with probability  $1 - C'n^{-2}$ .

Moreover, under mild assumptions it is shown in [32] that the residual estimation errors of  $\hat{\mathbf{X}}_M$  (suitably rotated) estimating  $\vec{\mathbf{I}}_m \otimes \mathbf{X}$  are row-wise asymptotically normal, providing a central-limit-theorem-like result for the estimation error.

## 1.2 Alignment and matching

An assumption that is made in most joint embedding (and joint inference) methodologies is that the graphs are *a priori* vertex-aligned; i.e., for each  $i \in [n]$ , vertex  $i$  represents the same entity in each of the  $m$  graphs; notable exceptions to this assumption include [30, 29, 56]. In situations where this is not the case, graph matching methods can be used to recover the true alignment before further inference is pursued. Graph matching is a broad term for the large collection of methods that are dedicated to finding an optimal alignment between the vertex sets of two (or more) networks; see the survey papers [46, 78, 13] for a review of the field. At its simplest, the problem of matching two  $n$ -vertex graphs can be cast as a special case of the quadratic assignment problem: Given graphs  $\mathbf{A}$  and  $\mathbf{B}$ , the graph matching problem seeks

to find all elements of  $\operatorname{argmin}_{P \in \Pi_n} \|\mathbf{A}P - P\mathbf{B}\|_F$  where  $\Pi_n$  is the set of  $n \times n$  permutation matrices. It is worth noting that if  $\mathbf{A}$  and  $\mathbf{B}$  are allowed to be weighted, directed, and loopy (i.e., with self-edges), then this is equivalent to the NP-hard quadratic assignment problem.

Due to its practical utility and computational complexity, there are a huge number of graph matching algorithms in the literature. Of note here are algorithms that provide high probability matching guarantees under different levels of network model complexity. Examples include recent work developing efficient methods for asymptotically perfect (and near-perfect) matching in correlated Erdős-Rényi graphs (e.g., both seeded [41, 36] and unseeded [39, 8, 18]). These algorithms often rely on *edge* correlation to be present across the graph pair: Edges within each graph are independent, and edges across graphs are independent with the exception that for each pair of vertices  $\{u, v\}$  (where for a graph  $\mathbf{A}$ ,  $E(\mathbf{A})$  denotes the set of edges in  $\mathbf{A}$ ):

$$\operatorname{corr}(\mathbb{1} \{\{u, v\} \in E(\mathbf{A})\}, \mathbb{1} \{\{u, v\} \in E(\mathbf{B})\}) = \rho_e > 0 \quad (3)$$

This correlation is necessary in the Erdős-Rényi and Stochastic Blockmodel settings (see [68, 14, 50, 51]) as in the Erdős-Rényi model all vertices are stochastically equivalent (and all vertices in each block are stochastically equivalent in the blockmodel setting). Indeed, in Erdős-Rényi graphs, if  $\mathbf{A}$  and  $\mathbf{B}$  are independent, then the probability

$$\mathbb{P}(Q \in \operatorname{argmin}_{P \in \Pi_n} \|\mathbf{A}P - P\mathbf{B}\|_F) \quad (4)$$

is the same for all  $Q \in \Pi_n$ .

When edge correlation is not present, matching must rely on structure across graphs for alignment. We note here the work in [74, 75] which establish algorithms for consistent ( $o(n)$  error for the graphon matching problem) matching across a pair of unseeded, uncorrelated latent position networks. The work in [74, 75] utilizes the common structure across latent spaces to match graphs. A similar thrust of work considers graph matching in random geometric graphs (see, for example, [65]), in which the signal in the geometry is used to match graphs without edge correlation, though our algorithmic approach and model is different than the work contained therein ([65], in particular, considered random complete dot-product graphs). In [21, 22], this structural correlation is termed the *heterogeneity* correlation across graphs, which combines with edge correlation to define the *total* correlation across graphs. To wit, for graphs  $\mathbf{A}$  and  $\mathbf{B}$  and permutation  $P$ , define

$$\Delta(\mathbf{A}, \mathbf{B}, P) = \frac{1}{2} \|\mathbf{A}P - P\mathbf{B}\|_F^2$$

We define the alignment strength (see [21]) between  $\mathbf{A}$  and  $\mathbf{B}$  under permutation  $P$  to be (where  $\delta_A = |E(\mathbf{A})|/\binom{n}{2}$  is the edge density of a graph)

$$\operatorname{str}(\mathbf{A}, \mathbf{B}, P) = \frac{\Delta(\mathbf{A}, \mathbf{B}, P)}{\frac{1}{n!} \sum_{Q \in \Pi_n} \Delta(\mathbf{A}, \mathbf{B}, Q)} = \frac{\Delta(\mathbf{A}, \mathbf{B}, P)/\binom{n}{2}}{\delta_A(1 - \delta_B) + \delta_B(1 - \delta_A)}$$

Alignment strength provides what its name suggests, a measure of the strength of the alignment across a pair of graphs. In [21, 22] it is empirically demonstrated that matching algorithms (there the SGM algorithm of [20]) perform better and faster when aligning graphs

with a higher alignment strength across them. They further note that if  $\mathbf{A}$  and  $\mathbf{B}$  are identically distributed with latent alignment  $P$ , then the alignment strength is asymptotically almost surely equivalent to the *total* correlation  $\rho_T$  across graphs (i.e.,  $\mathbf{str}(\mathbf{A}, \mathbf{B}, P) - \rho_T \xrightarrow{a.s.} 0$ ) where  $\rho_T$  is defined via  $\rho_T = 1 - (1 - \rho_e)(1 - \rho_h)$  where

- i.  $\rho_e$  is the edge-wise correlation defined in Eq. 3;
- ii.  $\rho_h$  is the heterogeneity correlation defined via  $\rho_h = \frac{\sigma^2}{\mu(1-\mu)}$ , where

$$\mathbf{P} = \mathbb{E}\mathbf{A} = [p_{uv}], \quad \mu = \sum_{\{u,v\} \in \binom{V}{2}} p_{uv} / \binom{n}{2}, \quad \sigma^2 := \sum_{\{u,v\} \in \binom{V}{2}} (p_{uv} - \mu)^2 / \binom{n}{2}.$$

Just as large values of alignment strength lead to better matching outcomes empirically, so too does larger total correlation. Of particular note is that total correlation can be (relatively) large even in the case where  $\rho_e = 0$ , as long as there is sufficient heterogeneity correlation.

### 1.3 Graph hypothesis testing

Graph hypothesis testing aims to determine whether two samples of graphs are generated from the same underlying distribution (the null hypothesis) or from different distributions (the alternative hypothesis). Researchers have proposed a range of methodologies and inferential techniques for graph hypothesis testing including the work in [23, 24, 71, 61, 58, 16]. In the context of RDPG's a (semiparametric) two sample graph hypothesis testing framework can be framed as follows. Given two mutually independent graph samples  $(\mathbf{A}^{(1)}, \dots, \mathbf{A}^{(k_1)}, \mathbf{X}) \sim \text{JRDPG}(F_X, n)$  and  $(\mathbf{B}^{(1)}, \dots, \mathbf{B}^{(k_2)}, \mathbf{Y}) \sim \text{JRDPG}(F_Y, n)$ , we consider the hypothesis testing problem:

$$\begin{aligned} H_0 : \mathbf{X} &\pm \mathbf{Y} \\ H_A : \mathbf{X} &\not\pm \mathbf{Y} \end{aligned}$$

where  $F_X \pm F_Y$  holds if there exist an orthogonal matrix  $\mathbf{W} \in \mathcal{O}_d$  such that  $\mathbf{X} = \mathbf{Y}\mathbf{W}$ . This accounts for the rotational non-identifiability of the latent positions in the RDPG model. Given estimated latent positions  $\hat{\mathbf{X}}$  and  $\hat{\mathbf{Y}}$  (computed, for example, via the ASE), there are a number of natural test statistics that can be formulated; for example, a scaled version of  $T = \|\hat{\mathbf{X}} - \hat{\mathbf{Y}}\mathbf{W}\|_F$  is used in [32, 58] and a scaled version of  $T = \|\hat{\mathbf{X}}\hat{\mathbf{X}}^T - \hat{\mathbf{Y}}\hat{\mathbf{Y}}^T\|_F$  is used in [56]. In the RDPG framework, suitable bootstrapping [33, 58] can be used to estimate the appropriate critical value and testing power.

Most existing testing methods assume that the nodes across graphs are perfectly aligned, and these methods cannot be readily applied when there are errors across labels. However, in many real-world applications the identity of nodes is often unknown, inconsistent, or partially observed, which leads to unaligned or partially aligned graphs. As discussed in 1.2, these errorful node correspondences can have a detrimental effect on testing power [56]. Defining the noisy test in this setting is nuanced. Considering the simplified setting where  $k_1 = k_2 = 1$ , let the potential label error be represented by a fraction, say  $\leq k/n$ , of the vertices being



shuffled. We then observe  $\mathbf{A}$  and  $\tilde{\mathbf{Q}}\mathbf{A}\tilde{\mathbf{Q}}^T$  for some  $\tilde{\mathbf{Q}} \in \Pi_{n,k} = \{\mathbf{P} \in \Pi_n : \text{tr}(\mathbf{P}) \geq n - k\}$ . For each  $\mathbf{Q} \in \Pi_{n,k}$ , the associated testing critical value is defined as the smallest value  $c_{\alpha,\mathbf{Q}}$  such that (where  $T$  is the appropriate test statistic)  $\mathbb{P}_{H_0}(T \geq c_{\alpha,\mathbf{Q}}) \leq \alpha$ . As the observed  $\tilde{\mathbf{Q}}$  is unknown, the conservative shuffled test would reject the null if  $T \geq \max_{\mathbf{Q} \in \Pi_{n,k}} c_{\alpha,\mathbf{Q}}$ ; this can result in lost testing power if  $c_{\alpha,\tilde{\mathbf{Q}}} < \max_{\mathbf{Q} \in \Pi_{n,k}} c_{\alpha,\mathbf{Q}}$  which can occur, for example, if  $\tilde{\mathbf{Q}}$  shuffles less than  $k/n$  fraction of the vertices [56]. When node alignments are not observed or properly recovered via graph matching, the underlying structural similarity between graphs may be obscured, and traditional testing methods can experience a significant loss of statistical power or inflated false positive rates.

## 2 OmniMatch

Our proposed matching methodology is designed for the setting where there is no edge correlation, significant heterogeneity correlation, and available seeded vertices. Here, *seeded vertices* refer to those vertices whose correspondence across graphs is known *a priori*. This amounts to optimizing over a restricted subspace of  $\Pi_n$  in which diagonal elements (those corresponding to the seeded vertices) of the unknown permutation are fixed to be 1. Notably, the **OmniMatch** algorithm can be used to align the unseeded vertices across any number  $m$  of networks.

Before stating the algorithm, we first introduce the problem set-up. Consider  $m$  vertex aligned graphs  $(\mathbf{A}^{(1)}, \mathbf{A}^{(2)}, \dots, \mathbf{A}^{(m)})$  on  $n = s + u$  vertices, though rather than observing these graphs, we observe networks where a portion of the vertices are potentially shuffled. To wit, suppose that the first  $s$  vertices are aligned across the  $m$  graphs and consider the remaining  $u$  vertices in each graph as having unknown correspondence across the collection; denote the aligned vertices via  $\mathcal{S}$  and the set of potentially shuffled vertices via  $\mathcal{U}$ . We shall model this missing correspondence via each graph being observed as

$$\mathbf{B}^{(i)} = (I_s \oplus \mathbf{Q}^{(i)})\mathbf{A}^{(i)}(I_s \oplus \mathbf{Q}^{(i)})^T,$$

and let the permutation associated with the permutation matrix  $\mathbf{Q}^{(i)} \in \mathbb{R}^{u \times u}$  be denoted  $\sigma^{(i)}$ . The **OmniMatch** algorithm proceeds as follows (see Algorithm 1 for **OmniMatch** pseudocode).

- i. Let the induced subgraph of  $\mathbf{B}^{(i)}$  on the  $s$  aligned vertices in  $\mathcal{S}$  be denoted  $\tilde{\mathbf{A}}^{(i)}$  with corresponding latent positions  $\tilde{\mathbf{X}}$ .
- ii. Embed the aligned vertices via  $\hat{\mathbf{X}}_M = \text{OMNI}(\tilde{\mathbf{A}}^{(1)}, \tilde{\mathbf{A}}^{(2)}, \dots, \tilde{\mathbf{A}}^{(m)}, d)$ . Let  $\hat{\mathbf{X}}_M^{(i)}$  denote the portion of  $\hat{\mathbf{X}}_M$  corresponding to graph  $i$  (i.e., rows  $[(i-1)*s+1] : [i*s]$ ). If the embedding dimension is unknown, it can be estimated via a number of available methods (e.g., [11]); we estimate the dimension via elbow-analysis of the SCREE plot based on [10, 77].
- iii. For each  $v \in \mathcal{U}$  and  $i \in [m]$  use the Least-Squares Out-Of-Sample (LLS OOS) embedding heuristic defined in [34] via

$$\hat{w}_{\sigma^{(i)}(v)} = \underset{w \in \mathbb{R}^d}{\text{argmin}} \sum_{j=1}^s \left( \vec{b}_v^{(i)} - \left( (\hat{\mathbf{X}}_M^{(i)})_j \right)^T w \right)^2 \quad (5)$$

to obtain the LLS OOS embedding  $\hat{w}_{\sigma^{(i)}(v)}$  of  $X_v$  in  $\mathbf{B}^{(i)}$ .

iv. For each  $i, j \in [m]$ , compute the cost matrices  $\mathbf{C}^{(i,j)} \in \mathbb{R}^{u \times u}$  where

$$\mathbf{C}_{v,w}^{(i,j)} = \|\hat{w}_{\sigma^{(i)}(v)} - \hat{w}_{\sigma^{(j)}(w)}\|^2.$$

v. For each  $i, j \in [m]$ , compute the matching of the unaligned vertices in  $\mathbf{B}^{(i)}$  to the unaligned vertices in  $\mathbf{B}^{(j)}$  by finding an element of

$$\operatorname{argmin}_{\mathbf{Q} \in \Pi_u} \operatorname{tr}(\mathbf{C}^{(i,j)} \mathbf{Q});$$

Solve the multidimensional assignment problem (MLAP see, for example, [43]) with cost matrices  $\{\mathbf{C}^{(i,j)}\}$  to find an assignment of labels to the unlabeled vertices across all  $m$  graphs. To wit, let the set of vertices with unknown labels in  $\mathbf{B}^{(i)}$  be denoted  $\mathcal{U}_{\mathbf{B}^{(i)}}$ , and for each  $\vec{v} = [v_i] \in \mathcal{U}_{\mathbf{B}^{(1)}} \times \mathcal{U}_{\mathbf{B}^{(2)}} \times \dots \times \mathcal{U}_{\mathbf{B}^{(m)}}$  define the cost

$$\mathcal{C}(\vec{v}) = \sum_{\{i,j\} \in \binom{[m]}{2}} \mathbf{C} \mathbf{C}_{v_i, v_j}^{(i,j)}.$$

We then seek permutations  $\pi_1, \dots, \pi_{m-1}$  to minimize the following cost

$$\sum_{v \in \mathcal{U}_{\mathbf{B}^{(1)}}} \mathcal{C}(v, \pi_1(v), \dots, \pi_{m-1}(v)).$$

This could be done with an off-the-shelf MLAP solver (such as in [43]); as an alternative, an anchor graph can be chosen and all other graphs aligned to the anchor pairwise. Solving the multidimensional assignment problem is NP-hard in general, when  $m = 2$  this amounts to solving a simple linear assignment problem which can be solved in  $O(u^3)$  time (using, for example, the Hungarian algorithm of [31]). Moreover, in the theoretical analysis below we can solve pairwise linear assignment problems

$$\operatorname{argmin}_{\mathbf{Q} \in \Pi_u} \operatorname{tr}(\mathbf{C}^{(i,j)} \mathbf{Q}) \tag{6}$$

and the composition of these assignments will, with probability going to 1, be internally consistent (i.e., if  $v \in \mathcal{U}_{\mathbf{B}^{(j)}}$  is mapped to  $w \in \mathcal{U}_{\mathbf{B}^{(l)}}$  and  $w \in \mathcal{U}_{\mathbf{B}^{(l)}}$  is mapped to  $z \in \mathcal{U}_{\mathbf{B}^{(h)}}$ , then  $v \in \mathcal{U}_{\mathbf{B}^{(j)}}$  will be mapped to  $z \in \mathcal{U}_{\mathbf{B}^{(h)}}$ ) and will provide the correct labels across all graphs.

## 2.1 Theoretical analysis

Herein, we provide theoretical analysis of the `Omnimatch` algorithm and prove our main algorithmic consistency result. Let  $(\mathbf{A}^{(1)}, \mathbf{A}^{(2)}, \dots, \mathbf{A}^{(m)}, \mathbf{X}) \sim \text{JRDPG}(F, n = s + u, m)$  where  $F$  is a distribution in  $\mathbb{R}^d$  satisfying the following Assumption.

**Assumption 1.** *We will assume the inner product distribution  $F$  further satisfies*



---

**Algorithm 1** OmniMatch for multiple seeded graph matching

---

**Require:** Graphs  $m$  graphs  $(\mathbf{B}^{(1)}, \mathbf{B}^{(2)}, \dots, \mathbf{B}^{(m)})$  each with  $n = s + u$  vertices; Seeded vertex set  $S$  assumed to be the same vertices  $S = \{1, 2, 3, \dots, s\}$  in each graph; Embedding dimension  $d$

**Ensure:** Alignment of unlabeled vertices across  $m$  graphs

- [i.] For each  $i \in [m]$ , let  $\tilde{\mathbf{A}}^{(i)} = \mathbf{A}^{(i)}[1 : s, 1 : s]$ ;
  - [ii.] Embed the aligned vertices via  $\hat{\mathbf{X}}_M = \text{OMNI}(\tilde{\mathbf{A}}^{(1)}, \tilde{\mathbf{A}}^{(2)}, \dots, \tilde{\mathbf{A}}^{(m)}, d)$ ;
  - [iii.] For each  $v \in \mathcal{U} = V \setminus S$  and  $i \in [m]$ , use the least-squares Out-of-sample embedding heuristic defined in Eq. 5 to obtain the LLS OOS embedding  $\hat{w}_{\sigma^{(i)}(v)}$  of  $X_v$  in  $\mathbf{B}^{(i)}$ ;
  - [iv.] For each  $i, j \in [m]$ , compute the cost matrices  $\mathbf{C}^{(i,j)} \in \mathbb{R}^{u \times u}$  where we define  $\mathbf{C}_{v,w}^{(i,j)} = \|\hat{w}_{\sigma^{(i)}(v)} - \hat{w}_{\sigma^{(j)}(w)}\|$ ;
  - [v.] Solve the multidimensional assignment problem with cost matrices  $\{\mathbf{C}^{(i,j)}\}$  to find an assignment of labels to the unlabeled vertices across all  $m$  graphs;
- 

- i. For all  $x, y \in \text{supp}(F)$ , there exists a constant  $\delta > 0$  such that  $\delta \leq x^T y \leq 1 - \delta$  (we denote this property as the  $\delta$ -inner product property);*
- ii. If  $\mathbf{Y} \sim F$ , then  $\mathbb{E}(\mathbf{Y}\mathbf{Y}^T)$  is rank  $d$ ;*
- iii. There exists a constant  $c_d > 0$  (depending on the latent dimension  $d$ , which is fixed) such that for any  $x \in \text{supp}(F)$ , we have that  $\mathbb{P}_F(X \in B_r(x)) \leq c_d r^d$ ; (this is not so onerous as the volume of the ball of radius  $r$  about  $x$  is proportional to  $r^d$ )*

Theorem 7 in [34], adapted here to account for the factor of  $m$  appearing in the Omnibus two-to-infinity bound yields that for the same  $\mathbf{W}$  as in Eq. 2, we have that (where  $X_v$  is the row of  $\mathbf{X}$  corresponding to vertex  $v$ ).

**Lemma 2.1.** *With notation and Assumption 1 on  $F$  as above, there exist constants  $D, D' > 0$ , rotation matrix  $\mathbf{W}$  (independent of out-of-sample-vertex  $v$  and graph index  $i$ ), and integer  $\mathfrak{s} > 0$  (all depending only on  $F$  and  $m$ ) such that for all  $s \geq \mathfrak{s}$ ,*

$$\|\hat{w}_{\sigma^{(i)}(v)} - \mathbf{W}^T X_v\|_2 \leq D \frac{m^{1/2} \log(ms)}{\sqrt{s}} \quad (7)$$

*holds with probability  $1 - D's^{-2}$ .*

Note that the  $\mathbf{W}$  appearing in Lemmas 1.1 and 2.1 can be taken to be equal.

Note that the non-asymptotic form of this Lemma (deviating from the “big-O” version in [34]; this is needed to apply a union bound over all  $v \in \mathcal{U}$  and over the  $m$  graphs) does require some nontrivial work; for the proof of the result, see Appendix A.1. Considering the bound in Eq. 7 uniformly over all  $u$  unknown vertices and all  $m$  graphs, we have that for all  $s \geq \mathfrak{s}$

$$\max_{i \in [m], v \in \mathcal{U}} \|\hat{w}_{\sigma^{(i)}(v)} - \mathbf{W}^T X_v\|_2 \leq \frac{Dm^{1/2} \log(ms)}{\sqrt{s}} \quad (8)$$

holds with probability at least  $1 - D'mus^{-2}$ .

We are now ready to state and prove our main result. With notation and assumptions as above, consider the **OmniMatch** algorithm where we output the solutions to the  $\binom{m}{2}$  LAP's in step [v]. as its final output. Our main result proves that this iteration of **OmniMatch** asymptotically almost surely perfectly aligns all unaligned vertices across all  $m$  graphs.

**Theorem 2.1.** *With notation and Assumption 1 as above, there exist constants  $D', D''$  and integer  $s'' > 0$  such that if  $s \geq s''$ , the probability that **OmniMatch** perfectly aligns the unaligned vertices across all  $m$  graph simultaneously is at least*

$$1 - p_{m,u,s,d} := 1 - D''m^{d/2}u^2 \frac{\log^{2d}(ms)}{s^{d/2}} - D'mus^{-2};$$

i.e., with probability at least  $1 - p_{m,u,s,d}$  we have that for all  $i, j \in [m]$ ,

$$\arg \min_{\mathbf{Q} \in \Pi_u} \text{tr}(\mathbf{C}^{(i,j)} \mathbf{Q}) = \{\mathbf{Q}^{(j)}(\mathbf{Q}^{(i)})^T\}.$$

Note that if  $u = s^\alpha$  for  $\alpha < \min(2, d/4)$  with  $m$  fixed, then Theorem 2.1 provides eventual perfect performance for **OmniMatch** with probability going to 1; note that the constants in the bounding probabilities do depend on  $d$ , and may be very large for moderate  $d$ . This asymptotically perfect matching is in spite of the fact that *there is no edge correlation* across any of the graphs in our collection. That said, the constraint on  $F$  and the dimension  $d$  (especially when  $d$  is modestly large) do provide a modest level of *total correlation* [21] across the networks—due to the presence of heterogeneity correlation across graphs—and this is enough to asymptotically perfectly align the vertices across networks.

*Proof of Theorem 2.1.* By assumption [iii]. on  $F$ , we have that if  $X, Y \stackrel{\text{ind.}}{\sim} F$ , then  $\mathbb{P}(\|X - Y\| \leq r) \leq c_d r^d$  (condition on  $X = x$  and apply assumption [iii]. to the probability  $Y$  falls into  $B_r(x)$ , integrating over  $x$  yields the result). We then have that ( $D$  here is the constant from Lemma 2.1)

$$\begin{aligned} & \mathbb{P}\left(\min_{v,w \in \mathcal{U}} \|X_v - X_w\| > \frac{10Dm^{1/2} \log^2(ms)}{\sqrt{s}}\right) \\ &= 1 - \mathbb{P}\left(\exists v, w \in \mathcal{U} \text{ s.t. } \|X_v - X_w\| \leq \frac{10Dm^{1/2} \log^2(ms)}{\sqrt{s}}\right) \\ &\geq 1 - c_d \binom{u}{2} \frac{10^d D^d m^{d/2} \log^{2d}(ms)}{s^{d/2}} \geq 1 - \xi_d u^2 m^{d/2} \frac{\log^{2d}(ms)}{s^{d/2}} \end{aligned} \quad (9)$$

for a suitable constant  $\xi_d > 0$ . Condition now on the events in Eq. 8 and Eq. 9 holding, and we see that

1. For all  $v \in \mathcal{U}$ , all OOS-embedded vertices corresponding to  $X_v$  are in a ball centered at  $\mathbf{W}^T X_v$  of radius  $\frac{Dm^{1/2} \log(ms)}{\sqrt{s}}$ ; this implies that

$$\max_{v \in \mathcal{U}} \max_{i,j \in [m]} \|\hat{w}_{\sigma(i)(v)} - \hat{w}_{\sigma(j)(v)}\| \leq 2 \frac{Dm^{1/2} \log(ms)}{\sqrt{s}} \quad (10)$$

2. For all  $v, w \in \mathcal{U}$ , the distance between  $X_v$  and  $X_w$  is at least  $\frac{10Dm^{1/2}\log^2(ms)}{\sqrt{s}}$ ; this implies that

$$\begin{aligned} \min_{v,w \in \mathcal{U}, v \neq w} \min_{i,j \in [m]} \|\hat{w}_{\sigma(i)(v)} - \hat{w}_{\sigma(j)(w)}\| &\geq \min_{v,w \in \mathcal{U}, v \neq w} \|X_v - X_w\| - 2 \max_{v \in \mathcal{U}} \max_{i \in [m]} \|\hat{w}_{\sigma(i)(v)} - X_v\| \\ &\geq 8 \frac{Dm^{1/2}\log(ms)}{\sqrt{s}} \end{aligned} \quad (11)$$

From Eqs. 10, 11, the perfect matching follows immediately as the Linear Assignment Problem cost matrix  $\mathbf{C}^{(i,j)}$  for matching graph  $\mathbf{B}^{(i)}$  to  $\mathbf{B}^{(j)}$  satisfies  $(\mathbf{Q}^{(i)})^T \mathbf{C}^{(i,j)} \mathbf{Q}^{(j)}$  has diagonal values uniformly dominated by  $2 \frac{Dm^{1/2}\log(ms)}{\sqrt{s}}$  and off-diagonal entries uniformly lower bounded by  $8 \frac{Dm^{1/2}\log(ms)}{\sqrt{s}}$ . It follows that the optimal matching is given by

$$\begin{aligned} \arg \min_{\mathbf{Q} \in \Pi_u} \text{tr}(\mathbf{C}^{(i,j)} \mathbf{Q}) &= \arg \min_{\mathbf{Q} \in \Pi_u} \text{tr}(\mathbf{Q}^{(i)} (\mathbf{Q}^{(i)})^T \mathbf{C}^{(i,j)} \mathbf{Q}^{(j)} (\mathbf{Q}^{(j)})^T \mathbf{Q}) \\ &= \arg \min_{\mathbf{Q} \in \Pi_u} \text{tr}((\mathbf{Q}^{(i)})^T \mathbf{C}^{(i,j)} \mathbf{Q}^{(j)} (\mathbf{Q}^{(j)})^T \mathbf{Q} \mathbf{Q}^{(i)}) = \{\mathbf{Q}^{(j)} (\mathbf{Q}^{(i)})^T\} \end{aligned}$$

as desired.  $\square$

### 3 Simulations And Real Data Experiments

Herein, we show the effectiveness of **OmniMatch** for both aligning graphs and as a preprocessing tool used prior to performing multiple graph hypothesis testing. For the code needed to run the experiments below, we refer the reader to <https://github.com/tong-qii/Omnimatch>.

#### 3.1 OmniMatch for graph matching

To evaluate the matching accuracy of the **OmniMatch** algorithm, we first generate vertex aligned graph pairs from the  $d$ -dimensional RDPG where the i.i.d. latent positions are obtained by projecting a  $\text{Dirichlet}(\vec{1}_{d+1})$  random vector onto the first  $d$  coordinates. We then shuffle a subset of the vertices in one graph (treating the remaining vertices as seeds), apply **OmniMatch** and compute the proportion of correctly aligned vertices. The adjacency matrices are generated with  $n = s + u = 500, 1000, 10000$  vertices, and we consider varying values of  $s$  and  $u$  for each  $n$ . The proportion of correctly matched vertices after shuffling and embedding is computed for two different variants of **OmniMatch**. The first method uses the “hard” matching approach presented above, where the estimated latent positions of the shuffled vertices are matched using a linear assignment solver. In this case, a shuffled vertex is correctly matched after unshuffling if it is exactly matched to its original position. The second method uses a “soft” matching approach (call this **S-OmniMatch**) where a shuffled vertex is correctly matched if its original unshuffled position is among the  $k$  nearest neighbors in the embedded space. In each case, for each choice of parameters, we average over  $nMC = 100$  simulations.

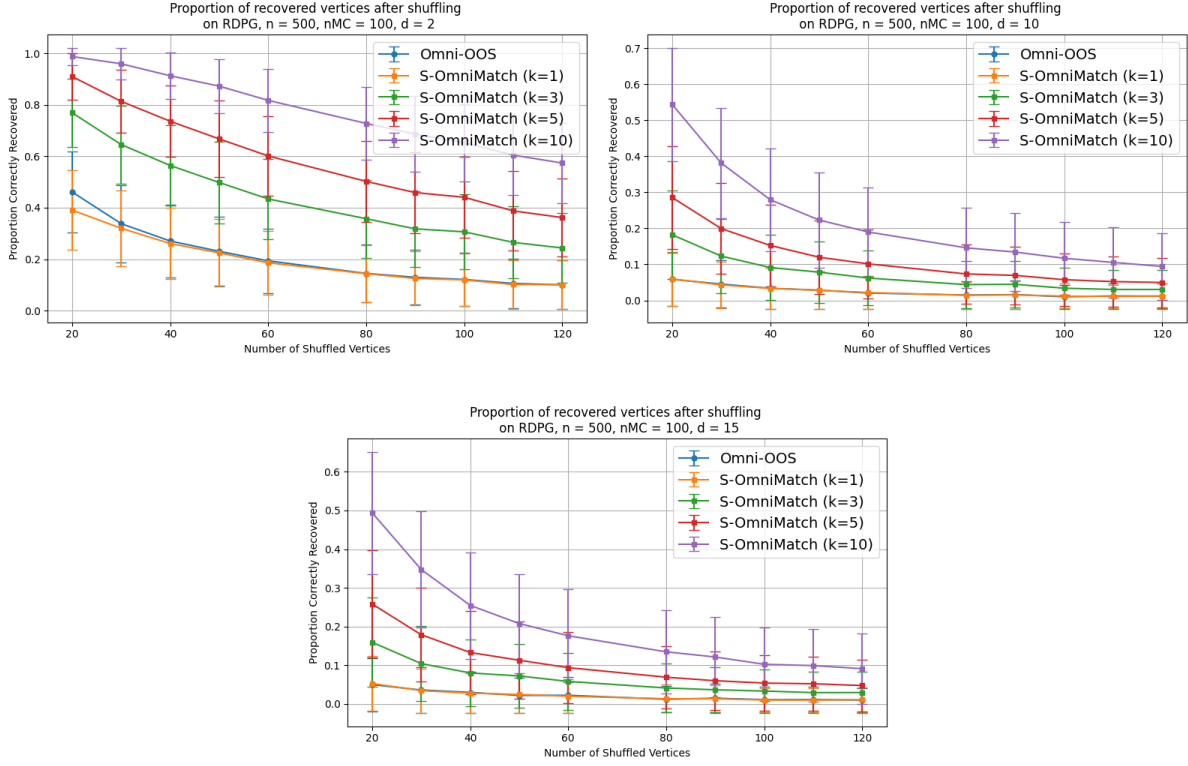


Figure 1: The proportion of correctly unshuffled vertices for **OmniMatch** and **S-OmniMatch** using the  $k = 1, 3, 5, 10$  nearest neighbors for two- (top-left), ten- (top-right) and fifteen-dimensional (bottom) RDPG with 500 vertices. Results are averaged over  $nMC = 100$  simulations.

In Figure 1 when  $n = 500$  vertices, we observe that **S-OmniMatch** performs about as well as or better than the hard-matching version of **OmniMatch** for all three dimensions of the embedding and all numbers of nearest neighbors ( $k = 1, 3, 5, 10$ ) in the embedded space. The proportion of correctly unshuffled vertices for **S-OmniMatch** increases with the number of neighbors, but decreases when the embedding dimension grows. The matching accuracy also decreases for **OmniMatch** as the dimension grows, and the accuracy is lower than for **S-OmniMatch** with  $k = 3, 5, 10$  nearest neighbors. We see a similar phenomena when  $n = 1000$ ; see Appendix B, Figure 8, for detail.

For larger networks with  $n = 10000$  vertices, we observe in Figure 2 that **S-OmniMatch** still outperforms the hard-matching **OmniMatch** for all dimensions, with only similar performance between **OmniMatch** and **S-OmniMatch** with  $k = 1$  nearest neighbor. We also observe an increased performance for both methods as the dimension is increased from two to ten, followed by a decrease as the dimension increases from ten to fifteen. This change in performance follows the trends in Figure 3. The precision seems to increase with  $k$  here; see Figure 9 in Appendix B. However, the methods have increasingly similar performance as the embedding dimension and number of nearest neighbors both increase. This is reasonable as the soft-matching method is overall more forgiving, and even more so when a larger number of nearest neighbors is considered for determining a correct match. Note that, in

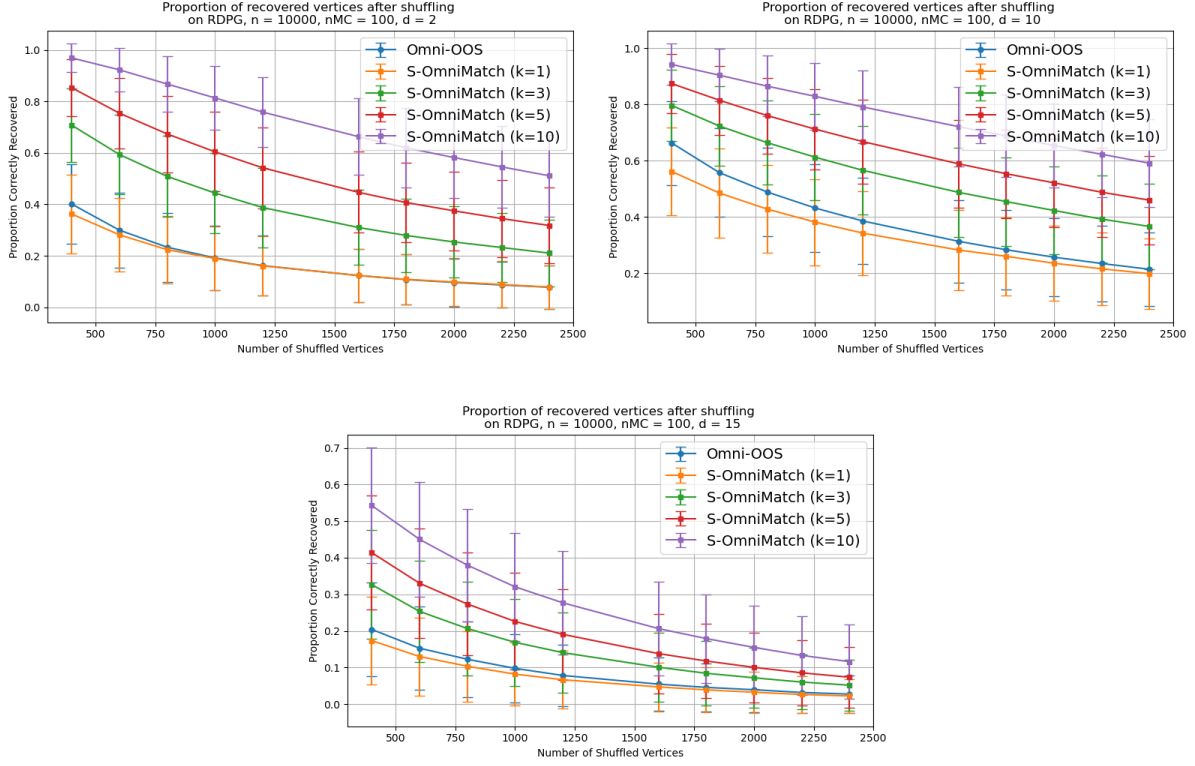


Figure 2: The proportion of correctly unshuffled vertices for **OmniMatch** and **S-OmniMatch** using the  $k = 1, 3, 5, 10$  nearest neighbors for two- (top-left), ten- (top-right) and fifteen-dimensional (bottom) RDPG with 10,000 vertices. Results are averaged over  $nMC = 100$  simulations.

this large graph setting, when we consider the effect of  $d$  on accuracy, we see in Figure 3 that for larger graphs, performance increases with  $d$  initially before decreasing for larger  $d$ . This coincides with our theory, as larger  $d$  allows for a better growth rate of  $u$  in terms of  $s$ , though the constants in our probability bounds often increase in  $d$  which eventually will inhibit performance given a fixed  $n$  and  $s$ .

### 3.1.1 OmniMatch for multiple graph matching

One application of graph matching is the computation of pairwise graph similarity: given a collection of unaligned (or partially aligned) networks, use graph matching tools to align the network and the graph matching objective function to assess the similarity of the networks. This matching objective function of Eq. 4 is a commonly occurring pseudo-distance [9] in the literature, and upper bounds the popular cut metric. Moreover, properly normalized, it is the root of the total correlation/alignment strength measure of graph similarity from [21]. To demonstrate the capability of **OmniMatch** to simultaneously align multiple graphs—and hence simultaneously provide similarity measures across a graph collection—we consider the following illustrative experiment based on multiple RDPGs. We generate 10 RDPGs from the same distribution, which posits i.i.d. latent positions from the Dirichlet( $\vec{1}_{12}$ ) distribution

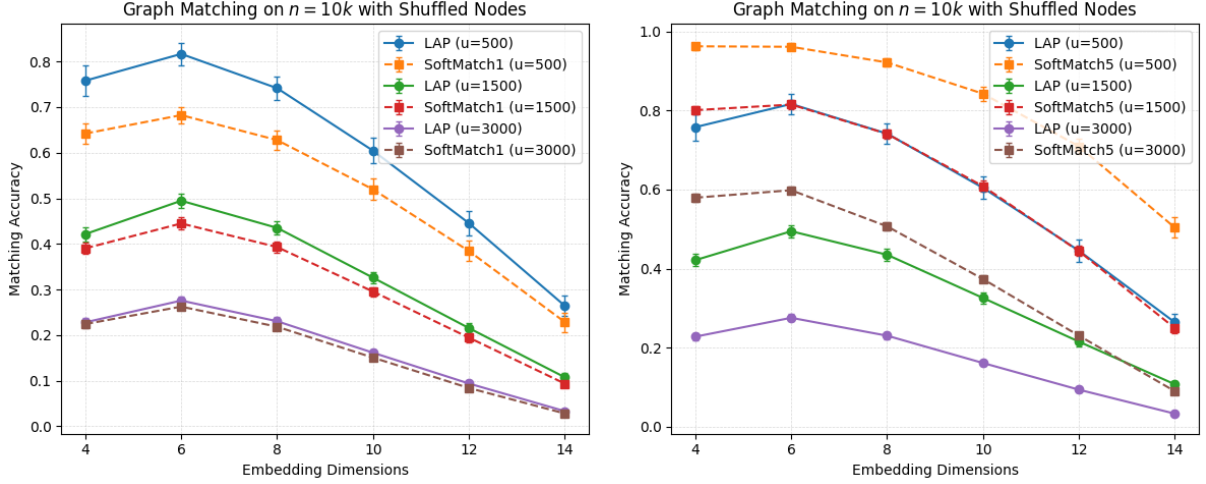
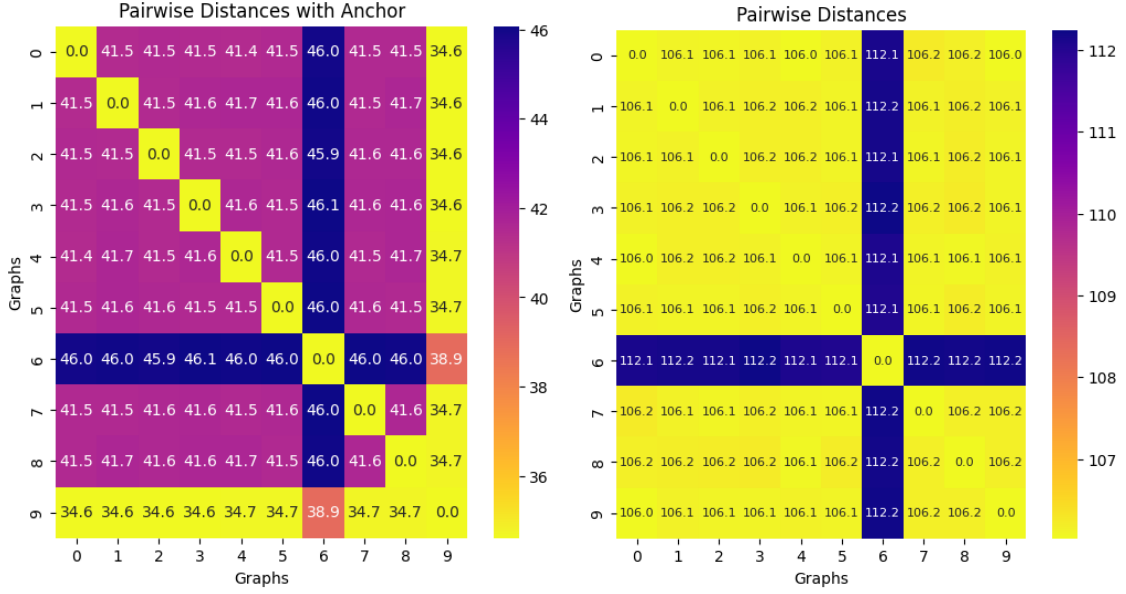


Figure 3: Graph matching accuracies on the graph with  $n = 10k$  nodes and  $n_s = [500, 1500, 3000]$  shuffled nodes using **OmniMatch** with LAP and **S-OmniMatch** with 1-nearest neighbor on the left panel. Results are averaged over  $nMC = 100$  simulations, the lines indicate the mean of the accuracies and the error bars represent one standard deviation. The right panel shows graph matching accuracies using **OmniMatch** with LAP and **S-OmniMatch** with 5-nearest neighbors.

projected onto the first  $d = 10$  coordinates. Each graph contains 500 nodes and we introduce  $u = 120$  (top) or  $u = 400$  (bottom) shuffled nodes for every graph (the same 120 or 400 shuffled in each graph, though the shuffling permutations differ graph-to-graph). To simulate errors, we randomly select one of the graphs and select 80 of its vertices at random; we then add errors into its probability matrix with  $\text{err} = 0.05$  on these vertices. Next, we apply **OmniMatch** to embed and align the shuffled vertices across the graphs and compute the graph matching objective function (i.e., the pairwise Frobenius distance among the aligned graphs), visualizing the results in the heatmaps of Figure 4. The left panels display the pairwise distances with the  $10^{\text{th}}$  graph as an anchor for **OmniMatch** (i.e., we align the embedded graphs by aligning each graph via the LAP to the  $10^{\text{th}}$  graph); the right panels show the pairwise distances without using an anchor graph, where **OmniMatch** is used to embed the graphs and each pairwise LAP alignment is performed. Both sets of heatmaps reveal significantly higher distance values for the graph where errors were introduced into the probability matrix, even in the case where the number of shuffled nodes is relatively high. Notably, the graphs where  $u = 400$  have higher values for the pairwise distances across the board, showing that in this case the matching we are finding may not be optimal (the matching in the  $u = 120$  case yields smaller values, though this is in a different embedding space), though it is sufficient to identify the anomalous graph here. This demonstrates the capacity of **OmniMatch** to align multiple graphs simultaneously and detect anomalies between the aligned collection.

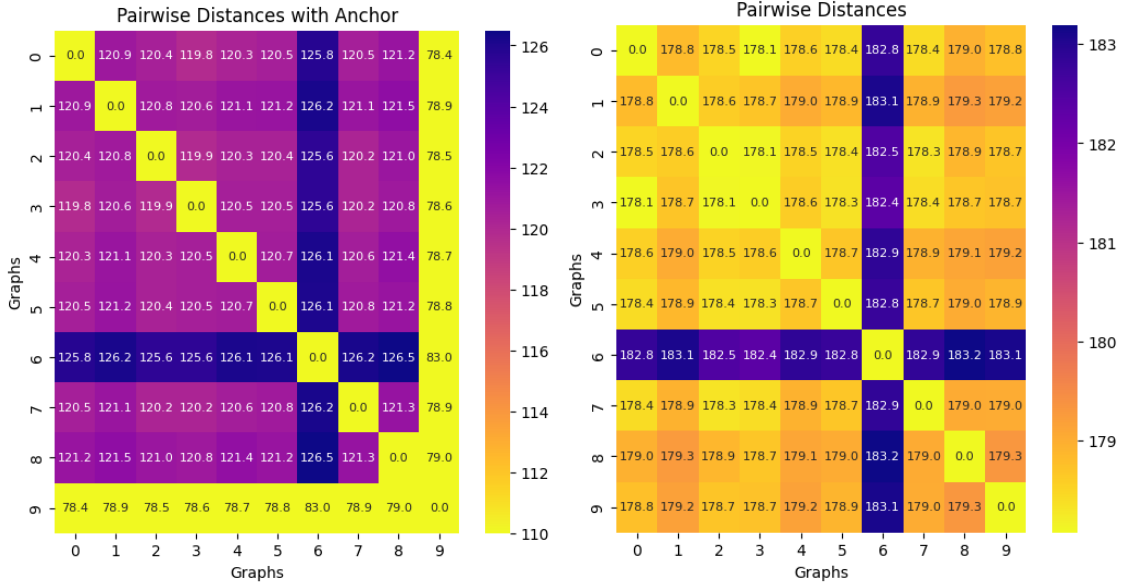
### 3.2 Power Test With Shuffling

We next aim to explore the effect of **OmniMatch** on two sample graph hypothesis testing. In the shuffled testing setting, one option is to use **OmniMatch** (and **S-OmniMatch**) as a preprocessing tool before applying more classical testing methods that assume known align-



(a) last graph as anchor graph,  $u = 120$

(b) without anchor graph (pairwise),  $u = 120$



(c) last graph as anchor graph,  $u = 400$

(d) without anchor graph (pairwise),  $u = 400$

Figure 4: Pairwise distances among 10 RDGP with  $n = 500$  nodes and  $u = 120$  (top) or  $u = 400$  (bottom) shuffled vertices using **OmniMatch**. The noise with  $\text{err} = 0.05$  is added to 80 randomly selected vertices in one randomly chosen graph. The left panels show pairwise distances computed using the last graph as an anchor. The right panels show pairwise distances computed without using any anchor graph.

ment *a priori*. Another option is to ignore the signal/noise in the labels across graphs and use a nonparametric (i.e., label free) testing procedure such as that proposed in [59, 3].



Similar to Section 3.1, we consider  $n = 500$  vertex RDPG’s, where under  $H_0$  the graphs are generated with i.i.d.  $\text{Dirichlet}(\vec{1}_{d+2})$  latent positions projected onto the first  $d$  coordinates. With notation as in Section 1.3 (here  $k_1 = k_2 = 1$ ), under the null hypothesis,  $\mathbf{A}$  is observed cleanly while  $v_0 = 120$  vertices of  $\mathbf{B}$  are shuffled. Under the alternative hypothesis,  $v_1 \in \{20, 30, 40, \dots, 100, 110, 120\}$  vertices are shuffled in  $\mathbf{B}$ . At the same time, a different scale of error is added to the latent positions  $\mathbf{Y} = \mathbf{X} + \text{err}$  as noise, where  $\text{err} = 0.01, 0.011, 0.012$ .

We employed two methods for the parametric tests. Graph pairs were generated with and without shuffled vertices corresponding the hard-matched **Omnimatch** and the soft-matching **S-Omnimatch** with  $k = 5$ ; in the soft-matched case the associated estimate for the soft-matched latent position is the average of these 5 soft-matched vertices. For both methods, the Frobenius norm between the latent position estimations of the whole graph pairs was computed as the test statistic (as in [32, 58]). We conducted  $nMC = 200$  rounds of simulation under the null and determined the 95<sup>th</sup> percentile of the null hypothesis distribution as the critical value. The power of the test was computed as the proportion of distances exceeding the critical value over the 200 simulations under the alternative model. We compare the performance of these two methods with the non-parametric test proposed in [59, 3], which is applied to pairs of graphs directly without need for pre-matching (this method estimates and compares the latent position distributions and do not use the labels across graphs) . All the embedding methods and tests are incorporated using **graspologic** Python package.

Results for  $d = 10$  are displayed in Figure 5 ; note that similar results hold when  $d = 2$  (see Figure 10 in Appendix B) though this higher embedding dimension setting allows for more structural information about the graphs to be preserved in the embedding space, leading to improved discriminative power. We see that, in general, **S-Omnimatch** outperforms **Omnimatch** across most parameter settings. Moreover, examining the plots column by column shows that soft matching with 5 nearest neighbors consistently achieves higher power compared to using 1 nearest neighbor; using 5 nearest neighbors achieves nearly optimal testing power across all parameter settings, and soft-matching has recovered the lost testing power. Moreover, the nonparametric method exhibits increasingly good power as  $\text{err}$  increases. This is entirely expected; what is of interest is that in these higher power settings, the matching-based tests (**S-Omnimatch** with  $k = 1$  and **Omnimatch**) are worse than the nonparametric tests in the overly conservative testing regime ( $v_1 < v_0$ ), though the testing power increases and surpasses the nonparametric alternative as  $v_1$  increases to  $v_0$ . Exploring this intersection point is of great interest, and is the subject of ongoing work.

### 3.3 Real Brain Data

We next include a real data set to examine the performance of **Omnimatch**. We consider a data set about connectomes that consists of 10 DTMRI brain scans for each of 30 subjects from the HNU1 data repository at [neurodata.io](https://neurodata.io). These connectomes data are produced with NeuroData’s MRI Graphs pipeline (m2g) [12]. Each scan is represented as a weighted graph with 70 vertices after being registered to the Desikan brain atlas. Each vertex corresponds to a region of interest (ROI) from the brain atlas and the edges between vertices indicate the strength of neuronal connections between these regions. All the graphs are pre-aligned both within individual subjects and across subjects.

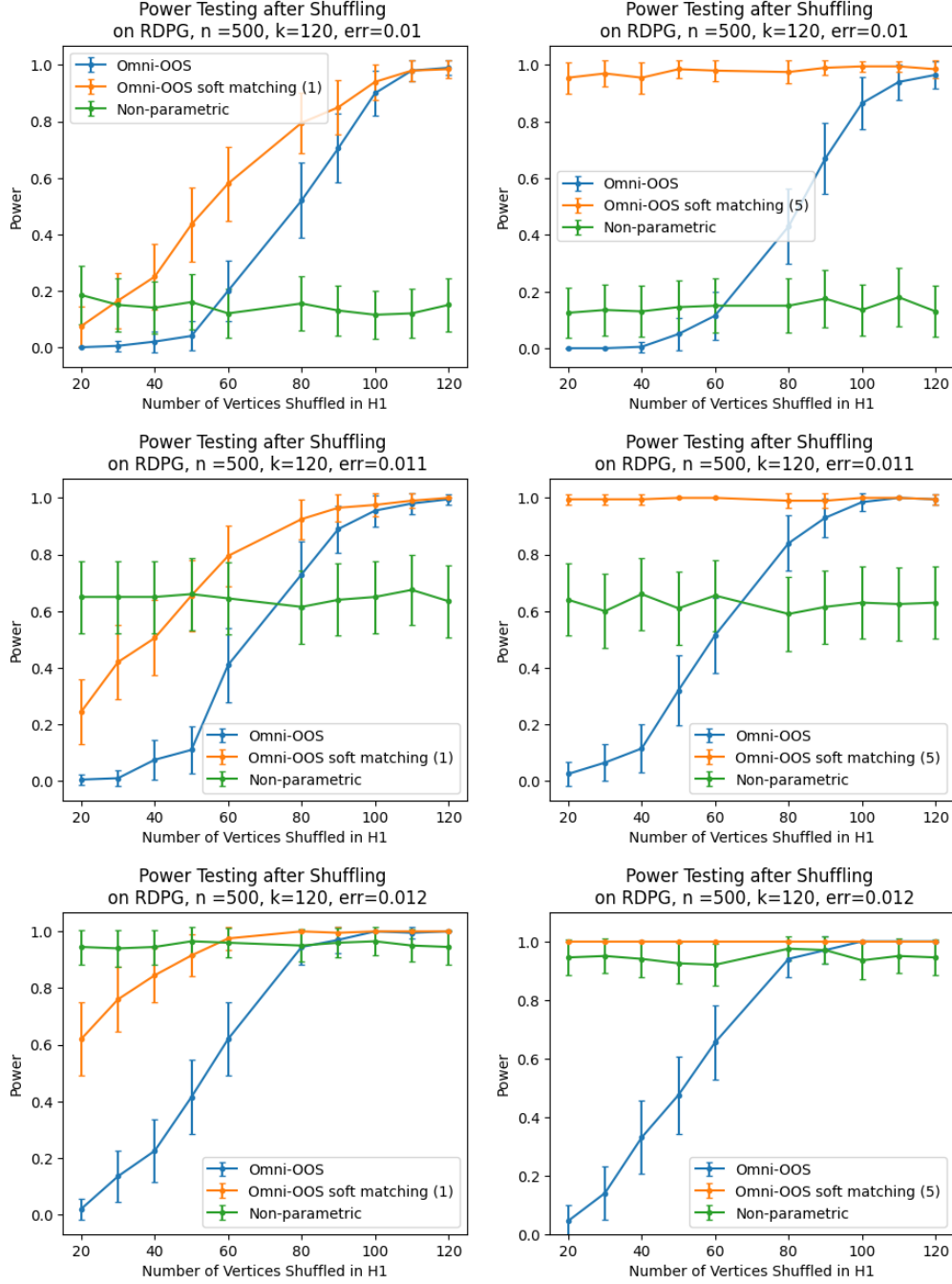


Figure 5: Statistical power for two-sample graph hypothesis testing under node shuffling. Each panel displays results from experiments on pairs of graphs with  $n = 500$  nodes. For each pair, one graph is fixed while the other has noise with  $\text{err} \in 0.01, 0.011, 0.012$  added to the lated positions. All embeddings are performed in dimension 10. The three panels on the left compare the empirical testing power of **OmniMatch**, **S-OmniMatch** using 1 nearest neighbor, and a non-parametric test. The three panels on the right include **S-OmniMatch** with 5 nearest neighbors.

In the experiments, we select the first 10 subjects, resulting in a total of 100 brain scans. Using the automatic dimensionality selection method (locating an appropriate elbow of the SCREE plot) based on [77, 10], we set the embedding dimension to  $dim = 7$  for these brain scan graphs. For this set of graphs, we randomly shuffled 20 or 50 vertices across all the graphs. We consider three approaches. We first directly apply the Omnibus embedding [32] to all 100 graphs with shuffled vertices (i.e., with no correction of the shuffling). This whole process is repeated for  $nMC = 200$  rounds, and the average pairwise distances are presented in the left column of Figure 6; note that in the heatmaps, the 100 graphs are ordered by subject, with each subject contributing 10 scans; thus the diagonal blocks correspond to within-subject comparisons. Lighter color blocks along the diagonal indicate that scans from the same subject exhibit shorter pairwise distances, reflecting higher similarity. The heatmaps on the middle column display the average pairwise distances after applying **Omnimatch** to align the vertices of all 100 brain scans, using the last brain scan as an anchor for vertex matching. The right column presents pairwise distance heatmaps obtained by applying **Omnimatch** with pairwise matching among the 100 brain scans. The top row in 6 corresponds to graphs with  $u = 20$  shuffled nodes, while the bottom row corresponds to  $u = 50$  shuffled nodes. Figure 6 clearly illustrates that the pairwise distances are lower when  $u = 20$  nodes are shuffled, compared to the case with  $u = 50$ . This effect is especially pronounced under the Omnibus embedding, where greater node misalignment significantly distorts the latent structure of the graphs, leading to increased dissimilarity across scans. However, in both the middle and right columns, the block structure becomes more distinct with sharper separation between different subjects. In particular, subjects with greater inter-scan variability, such as Subject 3 (scans from 31-40) and Subject 5 (scans from 51-60) exhibit more pronounced separation in the pairwise distance values. These results emphasize the effectiveness of **Omnimatch** in recovering meaningful graph structure and identifying variability to enhance interpretability within and across subjects in the presence of partial nodes shuffling.

To further evaluate the effectiveness of recovering subject-specific structure, we apply hierarchical clustering (**hclust**) to the pairwise distance matrices and compute the Adjusted Rand Index (ARI) for each trial. The ARI is a widely used statistical measure that quantifies the agreement between two clustering assignments. It ranges from -1 to 1, where a value near 0 suggests clustering similarity no better than random chance, while a value of 1 indicates a perfect match between the predicted and true cluster assignments. We perform **hclust** using the complete linkage method in Python which defines the distance between clusters as the maximum pairwise distance between their elements. Clusters are formed using the **maxclust** criterion and a target of 10 clusters for 10 subjects from the data. The whole process is repeated for  $nMC = 200$  simulations to compute the averages. The results of this evaluation are summarized in Table 1. For both  $u = 20$  and  $u = 50$ , the **Omnimatch** method applied with pairwise node matching consistently achieves the highest ARI scores, followed by **Omnimatch** with anchor graph. When the proportion of shuffled nodes is relatively small ( $u = 20$ ), OMNI retains enough structural information to support accurate clustering. However, as the number of shuffled nodes increases to  $u = 50$ , the performance of OMNI degrades significantly. In contrast, **Omnimatch** remains robust and continues to deliver high clustering accuracy, as reflected by its higher ARI values across both settings.

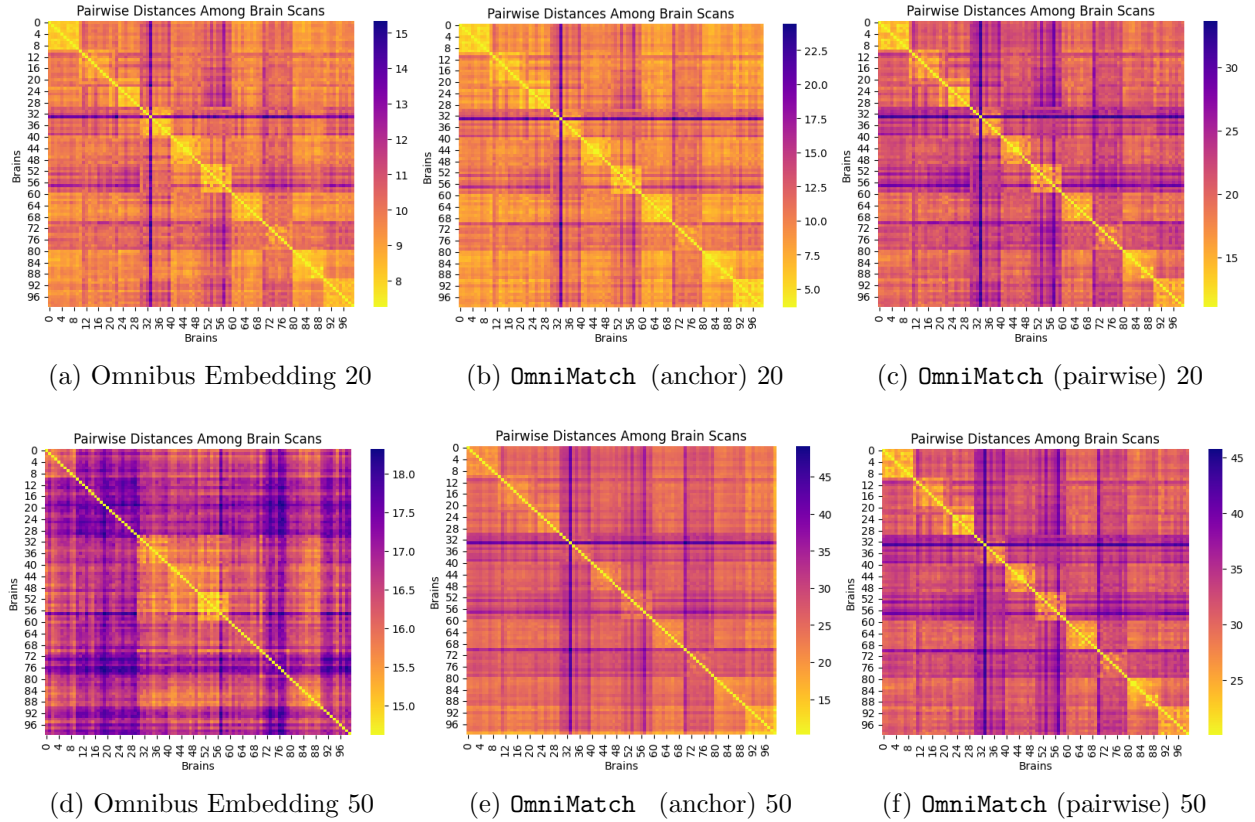


Figure 6: Pairwise distance heatmaps among 100 brain scans. A total of 10 subjects, each with 10 brain scan derived graphs are included for embedding. The left column displays the mean pairwise distances computed via the Omnibus Embedding procedure, the middle column presents the mean pairwise distances averaged over  $nMC = 200$  simulations involving application of **OmniMatch** using the last brain scan as anchor to match the vertices. The right column utilizes **OmniMatch** on pairwise nodes matching. The top and bottom row have  $u = 20$  and  $u = 50$  randomly shuffled nodes per graph respectively.

Algorithm	OMNI	<b>OmniMatch</b> (anchor)	<b>OmniMatch</b> (pairwise)
avg(ARI) 20	0.2897	0.4374	0.5132
avg(ARI) 50	0.0199	0.2525	0.4229

Table 1: Mean Adjusted Rand Index (ARI) over  $nMC = 200$  simulations for clustering brain scan graphs under OMNI and **OmniMatch** alignment methods and levels of node shuffling. Results are reported for  $u = 20$  and  $u = 50$  randomly shuffled nodes. **OmniMatch** with pairwise matching consistently achieves the highest ARI, demonstrating greater robustness to node misalignment.

### 3.4 **OmniMatch** applied to English-Zulu Parallel Sentences

We further conduct experiments on a cross-lingual dataset consisting of 1000 English sentences and their corresponding translations into Zulu. Sentence embeddings were obtained

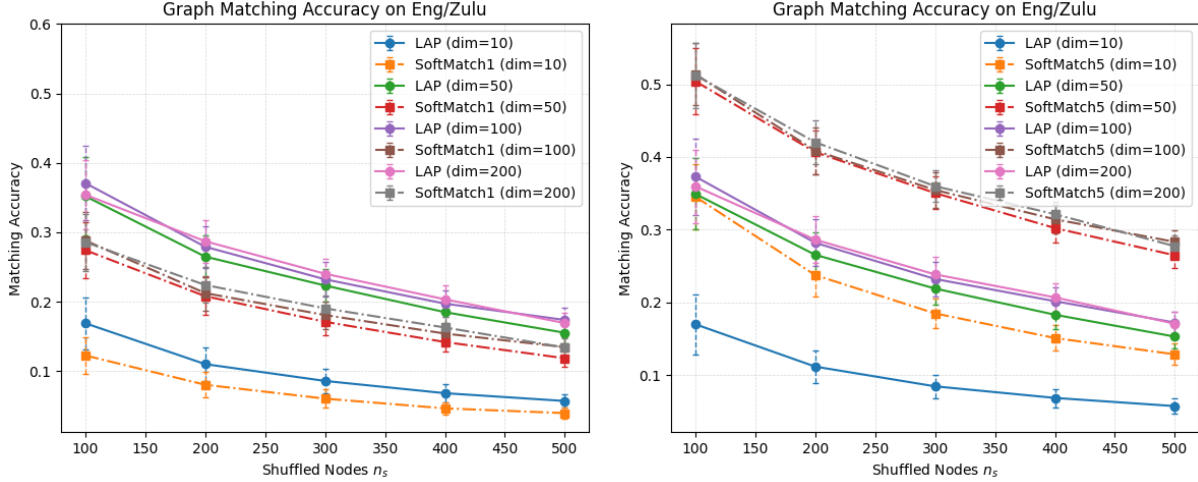


Figure 7: Graph matching accuracies for both LAP and S-OmniMatch on English Zulu data. The left panel presents the mean matching accuracies using S-OmniMatch with 1-nearest neighbor for matching. The right panel displays results using 5-nearest neighbor for matching. The accuracies are average over  $nMC = 200$  simulations. The number of shuffled nodes varies as  $u = [100, 200, 300, 400, 500]$  and the embedding dimensions varies as  $d = [10, 50, 100, 200]$ .

using the Nomic embedding framework [45], applied to the raw textual data. The resulting datasets for both English and Zulu consist of matrices of size  $1000 \times 768$ , where each row corresponds to the 768 dimensional embedding of a sentence. For each language, we compute the pairwise cosine similarity matrices and use them as input to both the OmniMatch and S-OmniMatch algorithms. This results in  $m = 2$  graphs whose vertices/nodes are  $n=1000$  sentences, each of which has a corresponding translation in the other graph. The edges are inferred sentence-level measures of semantic similarity computed in the embedding spaces. Following a similar experimental setup as described in Section 3.1, we evaluate matching performance under varying levels of node shuffling, with the number of shuffled nodes set to  $u = [100, 200, 300, 400, 500]$  embedding dimensions chosen from  $dim = [10, 50, 100, 200]$ . Here a correct match corresponds to recovering the correct out-of-sample embedded Zulu translation for each out-of-sample embedded English sentence. Each configuration is repeated over  $nMC = 200$  simulations, and the average matching accuracies are computed and visualized in Fig. 7.

The left panel of Fig. 7 presents the average graph matching accuracies using OmniMatch and S-OmniMatch with 1-nearest neighbor matching. In this setting, the hard matched linear alignment (LAP) consistently achieves higher accuracy across all levels of node shuffling. In contrast, the right panel displays results for 5-nearest neighbor matching using S-OmniMatch, where the soft matching approach consistently outperforms LAP, demonstrating its effectiveness in leveraging neighborhood information for more robust alignment under higher uncertainty. The original data here is 768 dimensional. We see here that performance increases for all  $d$  considered, though  $d = 100$  and  $d = 200$  show similar performance. This suggests that the data is most likely truly high dimensional, though there appears to be a diminishing return when including many data dimensions.



## 4 Discussion

In this work, we propose **Omnimatch** to address the challenge of partial node scrambling in graphs, where efficient graph node matching and two-sample graph hypothesis testing must be performed under node permutation uncertainty. This scenario frequently arises in practical applications such as social networks and biological network data, where perfect node alignment cannot be assumed. Most existing graph inference methods rely on the assumption of known node correspondences, thereby limiting their applicability when alignment is unknown. To overcome this limitation, **Omnimatch** integrates joint embedding and approximate graph matching under the setting of independent edge correlations, enabling both node correspondence recovery and robust hypothesis testing across graph pairs. Leveraging the RDPG model and the Omnibus embedding framework, **Omnimatch** extends latent positions to out-of-sample nodes and formulates an approximate graph matching problem that can be efficiently solved. The proposed method generalizes beyond pairwise alignment to accommodate the joint matching of multiple ( $m > 2$ ) graphs, enabling simultaneous alignment across networks. We theoretically establish the consistency of **Omnimatch** under general conditions, ensuring its robustness and reliability for a wide range of graph inference tasks.

Through comprehensive simulation results and real world data analysis, we demonstrated **Omnimatch** effectively recovers node alignments, improves the power of two-sample tests under varying levels of node shuffling and embedding dimensions, and practically distinguish the graph with disorganized nodes among a collection of graphs. Moreover, it has practical application to problems of harvesting NLP data, such as scraping and aligning parallel sentence pairs from web documents which contain similar content in different languages [7]. The results underline the necessity of integrating graph matching with joint embedding on statistical testing when addressing node misalignment. Extending the current framework to fully unaligned structure, dynamic temporal networks or graphs with varying sizes still desire further investigation. Additionally, optimizing the embedding dimension selection and improving computational scalability for very large graphs applications are also critical for broader applications.

### Acknowledgments

The authors gratefully acknowledge the support of the JHU Human Language Technology Center of Excellence, especially Paul McNamee and Kevin Duh. The English-Zulu sentence pairs are taken from the Opus machine translation data portal.[62]

## References

- [1] J. Agterberg, M. Tang, and C. E. Priebe. On two distinct sources of nonidentifiability in latent position random graph models. *arXiv preprint arXiv:2003.14250*, 2020.
- [2] Joshua Agterberg and Anru Zhang. Statistical inference for low-rank tensors: Heteroskedasticity, subgaussianity, and applications. *arXiv preprint arXiv:2410.06381*, 2024.

- [3] A. A. Alyakin, J. Agterberg, H. S. Helm, and C. E. Priebe. Correcting a nonparametric two-sample graph hypothesis test for graphs with different numbers of vertices with applications to connectomics. *Applied Network Science*, 9(1):1, 2024.
- [4] J. Arroyo, A. Athreya, J. Cape, G. Chen, Priebe C. E., and J. T. Vogelstein. Inference for multiple heterogeneous networks with a common invariant subspace. *Journ. of Mach. Learn. Res.*, 22:1–49, 2021.
- [5] D. Asta and C. R. Shalizi. Geometric network comparison. In M. Meila and T. Haskes, editors, *Proc. of the 31st Conf. on Uncertainty in Artificial Intelligence*, pages 102–110, 2015.
- [6] A. Athreya, D. E. Fishkind, K. Levin, , V. Lyzinski, Y. Park, Y. Qin, D. L. Sussman, M. Tang, J. T. Vogelstein, and C. E. Priebe. Statistical inference on random dot product graphs: a survey. *Journal of Machine Learning Research*, 18, 2018.
- [7] Marta Bañón, Pinzhen Chen, Barry Haddow, Kenneth Heafield, Hieu Hoang, Miquel Esplà-Gomis, Mikel L. Forcada, Amir Kamran, Faheem Kirefu, Philipp Koehn, Sergio Ortiz Rojas, Leopoldo Pla Sempere, Gema Ramírez-Sánchez, Elsa Sarriás, Marek Str-elec, Brian Thompson, William Waites, Dion Wiggins, and Jaume Zaragoza. ParaCrawl: Web-scale acquisition of parallel corpora. In Dan Jurafsky, Joyce Chai, Natalie Schluter, and Joel Tetreault, editors, *Proceedings of the 58th Annual Meeting of the Association for Computational Linguistics*, pages 4555–4567, Online, July 2020. Association for Computational Linguistics.
- [8] B. Barak, C. Chou, Z. Lei, T. Schramm, and Y. Sheng. (nearly) efficient algorithms for the graph matching problem on correlated random graphs. *Adv. in Neural Infor. Proc. Sys.*, 32:9190–9198, 2019.
- [9] J. Bento and S. Ioannidis. A family of tractable graph distances. In *Proceedings of the 2018 SIAM International Conference on Data Mining*, pages 333–341. SIAM, 2018.
- [10] S. Chatterjee. Matrix estimation by universal singular value thresholding. *The Annals of Statistics*, 43:177–214, 2014.
- [11] Fan Chen, Sebastien Roch, Karl Rohe, and Shuqi Yu. Estimating graph dimension with cross-validated eigenvalues. *arXiv preprint arXiv:2108.03336*, 2021.
- [12] J. Chung, R. Lawrence, A. Loftus, D. Pisner, G. Kiar, E. W. Bridgeford, W. G. Roncal, Consortium for Reliability, Reproducibility (CoRR), V. Chandrashekhhar, D. Mhem-bere, et al. A low-resource reliable pipeline to democratize multi-modal connectome estimation and analysis. *bioRxiv*, pages 2021–11, 2021.
- [13] D. Conte, P. Foggia, C. Sansone, and M. Vento. Thirty years of graph matching in pattern recognition. *Int. journal of pattern recognition and artificial intelligence*, 18(03):265–298, 2004.



- [14] D. Cullina and N. Kiyavash. Improved achievability and converse bounds for erdos-rényi graph matching. *ACM SIGMETRICS Performance Evaluation Review*, 44(1):63–72, 2016.
- [15] D. Cullina and N. Kiyavash. Exact alignment recovery for correlated erdos renyi graphs. *arXiv preprint arXiv:1711.06783*, 2017.
- [16] Xinjie Du and Minh Tang. Hypothesis testing for equality of latent positions in random graphs. *Bernoulli*, 29(4):3221–3254, 2023.
- [17] Frank Emmert-Streib, Matthias Dehmer, and Yongtang Shi. Fifty years of graph matching, network alignment and network comparison. *Information sciences*, 346:180–197, 2016.
- [18] Z. Fan, C. Mao, Y. Wu, and J. Xu. Spectral graph matching and regularized quadratic relaxations: Algorithm and theory. In *Int. Conf. on Machine Learning*, pages 2985–2995. PMLR, 2020.
- [19] Emily S Finn, Xilin Shen, Dustin Scheinost, Monica D Rosenberg, Jessica Huang, Marvin M Chun, Xenophon Papademetris, and R Todd Constable. Functional connectome fingerprinting: identifying individuals using patterns of brain connectivity. *Nature neuroscience*, 18(11):1664–1671, 2015.
- [20] D. E. Fishkind, S. Adali, H. G. Patsolic, L. Meng, D. Singh, V. Lyzinski, and C. E. Priebe. Seeded graph matching. *Pattern recognition*, 87:203–215, 2019.
- [21] D. E. Fishkind, L. Meng, A. Sun, C. E. Priebe, and V. Lyzinski. Alignment strength and correlation for graphs. *Pattern Recognition Letters*, 125:295–302, 2019.
- [22] D. E. Fishkind, F. Parker, H. Sawczuk, L. Meng, E. Bridgeford, A. Athreya, C. Priebe, and V. Lyzinski. The phantom alignment strength conjecture: practical use of graph matching alignment strength to indicate a meaningful graph match. *Applied Network Science*, 6(1):1–27, 2021.
- [23] Debarghya Ghoshdastidar, Maurilio Gutzeit, Alexandra Carpentier, and Ulrike Von Luxburg. Two-sample hypothesis testing for inhomogeneous random graphs. *The Annals of Statistics*, 48(4):2208–2229, 2020.
- [24] Debarghya Ghoshdastidar and Ulrike Von Luxburg. Practical methods for graph two-sample testing. *Advances in Neural Information Processing Systems*, 31, 2018.
- [25] G. H. Golub and C. F. Van Loan. *Matrix computations*. JHU press, 2013.
- [26] N. A. Heard, D. J. Weston, K. Platanioti, and D. J. Hand. Bayesian anomaly detection methods for social networks. *Annals of Applied Statistics*, 4:645–662, 2010.
- [27] P. D. Hoff, A. E. Raftery, and M. S. Handcock. Latent space approaches to social network analysis. *Journal of the American Statistical Association*, 97(460):1090–1098, 2002.

- [28] Bing-Yi Jing, Ting Li, Zhongyuan Lyu, and Dong Xia. Community detection on mixture multi-layer networks via regularized tensor decomposition. *arXiv preprint arXiv:2002.04457*, 2020.
- [29] N. Josephs, W. Li, and E. D. Kolaczyk. Network recovery from unlabeled noisy samples. In *2021 55th Asilomar Conference on Signals, Systems, and Computers*, pages 1268–1273. IEEE, 2021.
- [30] E. D. Kolaczyk, L. Lin, S. Rosenberg, J. Walters, and J. Xu. Averages of unlabeled networks: Geometric characterization and asymptotic behavior. *Ann. Statist.* 48(1): 514–538, 2020.
- [31] H. W. Kuhn. The Hungarian method for the assignment problem. *Naval Research Logistic Quarterly*, 2:83–97, 1955.
- [32] K. Levin, A. Athreya, M. Tang, V. Lyzinski, Y. Park, and C. E. Priebe. A central limit theorem for an omnibus embedding of multiple random graphs and implications for multiscale network inference. *arXiv preprint arXiv:1705.09355*, 2017.
- [33] K. Levin and E. Levina. Bootstrapping networks with latent space structure. *Electronic Journal of Statistics*, 19(1):745–791, 2025.
- [34] K. D. Levin, F. Roosta, M. Tang, M. W. Mahoney, and C. E. Priebe. Limit theorems for out-of-sample extensions of the adjacency and laplacian spectral embeddings. *Journal of Machine Learning Research*, 22(194):1–59, 2021.
- [35] V. Lyzinski. Information recovery in shuffled graphs via graph matching. *IEEE Transactions on Information Theory*, 64(5):3254–3273, 2018.
- [36] V. Lyzinski, D.E. Fishkind, and C.E. Priebe. Seeded graph matching for correlated Erdős-Rényi graphs. *Journ. of Mach. Learn. Res.*, 15:3513–3540, 2014.
- [37] V. Lyzinski, D. L. Sussman, M. Tang, A. Athreya, and C. E. Priebe. Perfect clustering for stochastic blockmodel graphs via adjacency spectral embedding. *Electronic Journal of Statistics*, 8:2905–2922, 2014.
- [38] Vince Lyzinski, Sancar Adali, Joshua T Vogelstein, Youngser Park, and Carey E Priebe. Seeded graph matching via joint optimization of fidelity and commensurability. *stat*, 1050:16, 2014.
- [39] Cheng Mao, Yihong Wu, Jiaming Xu, and Sophie H Yu. Random graph matching at otter’s threshold via counting chandeliers. In *Proceedings of the 55th Annual ACM Symposium on Theory of Computing*, pages 1345–1356, 2023.
- [40] Kelly Marchisio, Ali Saad-Eldin, Kevin Duh, Carey Priebe, and Philipp Koehn. Bilingual lexicon induction for low-resource languages using graph matching via optimal transport. In Yoav Goldberg, Zornitsa Kozareva, and Yue Zhang, editors, *Proceedings of the 2022 Conference on Empirical Methods in Natural Language Processing*, pages 2545–2561, Abu Dhabi, United Arab Emirates, December 2022. Association for Computational Linguistics.

- [41] E. Mossel and J. Xu. Seeded graph matching via large neighborhood statistics. *Random Structures & Algorithms*, 57(3):570–611, 2020.
- [42] Mark EJ Newman, Duncan J Watts, and Steven H Strogatz. Random graph models of social networks. *Proceedings of the national academy of sciences*, 99(suppl\_1):2566–2572, 2002.
- [43] D. M. Nguyen, Hoai A. Le T., and T. Pham Dinh. Solving the multidimensional assignment problem by a cross-entropy method. *Journal of Combinatorial Optimization*, 27:808–823, 2014.
- [44] Majid Noroozi and Marianna Pensky. Sparse subspace clustering in diverse multiplex network model. *Journal of Multivariate Analysis*, 203:105333, 2024.
- [45] Zach Nussbaum, John X Morris, Brandon Duderstadt, and Andriy Mulyar. Nomic embed: Training a reproducible long context text embedder. *arXiv preprint arXiv:2402.01613*, 2024.
- [46] S. J. Pan and Q. Yang. A survey on transfer learning. *IEEE Trans. Know. and Data Eng.*, 22(10):1345–1359, 2010.
- [47] K. Pantazis, A. Athreya, J. Arroyo, W. N. Frost, E. S. Hill, and V. Lyzinski. The importance of being correlated: Implications of dependence in joint spectral inference across multiple networks. *Journal of Machine Learning Research*, 23(141):1–77, 2022.
- [48] Marianna Pensky and Teng Zhang. Spectral clustering in the dynamic stochastic block model. *Electron. J. Statist.*, 13(1):678–709, 2019.
- [49] C. E. Priebe, Y. Park, J. T. Vogelstein, J. M. Conroy, V. Lyzinski, M. Tang, A. Athreya, J. Cape, and E. Bridgeford. On a two-truths phenomenon in spectral graph clustering. *Proceedings of the National Academy of Sciences*, 116(13):5995–6000, 2019.
- [50] M. Racz and A. Sridhar. Correlated stochastic block models: Exact graph matching with applications to recovering communities. *Adv. in Neural Infor. Proc. Sys.*, 34, 2021.
- [51] Miklós Z Rácz and Anirudh Sridhar. Matching correlated inhomogeneous random graphs using the k-core estimator. In *2023 IEEE International Symposium on Information Theory (ISIT)*, pages 2499–2504. IEEE, 2023.
- [52] Jesús D Arroyo Relión, Daniel Kessler, Elizaveta Levina, and Stephan F Taylor. Network classification with applications to brain connectomics. *The annals of applied statistics*, 13(3):1648, 2019.
- [53] K. Rohe, S. Chatterjee, and B. Yu. Spectral clustering and the high-dimensional stochastic blockmodel. *Annals of Statistics*, 39:1878–1915, 2011.
- [54] W. G. Roncal, Z. H. Koterba, D. Mhembere, D. M. Kleissas, J. T. Vogelstein, R. Burns, A. R. Bowles, D. K. Donavos, S. Ryman, R. E. Jung, et al. Migraine: Mri graph reliability analysis and inference for connectomics. In *2013 IEEE global conference on signal and information processing*, pages 313–316. IEEE, 2013.

- [55] P. Rubin-Delanchy, J. Cape, M. Tang, and C. E. Priebe. A statistical interpretation of spectral embedding: the generalised random dot product graph. *Journal of the Royal Statistical Society Series B: Statistical Methodology*, 84(4):1446–1473, 2022.
- [56] A. Saxena and V. Lyzinski. Lost in the shuffle: Testing power in the presence of errorful network vertex labels. *Computational Statistics & Data Analysis*, 204:108091, 2025.
- [57] D. L. Sussman, M. Tang, D. E. Fishkind, and C. E. Priebe. A consistent adjacency spectral embedding for stochastic blockmodel graphs. *Journ. of the American Statistical Association*, 107(499):1119–1128, 2012.
- [58] M. Tang, A. Athreya, D. L. Sussman, V. Lyzinski, Y. Park, and C. E. Priebe. A semiparametric two-sample hypothesis testing problem for random dot product graphs. *Journal of Computational and Graphical Statistics*, 26:344–354, 2017.
- [59] M. Tang, A. Athreya, D. L. Sussman, V. Lyzinski, and C. E. Priebe. A nonparametric two-sample hypothesis testing problem for random dot product graphs. *Bernoulli*, 23:1599–1630, 2017.
- [60] M. Tang, D. L. Sussman, and C. E. Priebe. Universally consistent vertex classification for latent position graphs. *Annals of Statistics*, 41:1406 – 1430, 2013.
- [61] Minh Tang, Avanti Athreya, Daniel L Sussman, Vince Lyzinski, and Carey E Priebe. A nonparametric two-sample hypothesis testing problem for random graphs. *Bernoulli* 23(3): 1599-1630, 2017.
- [62] Jörg Tiedemann. OPUS – parallel corpora for everyone. In *Proceedings of the 19th Annual Conference of the European Association for Machine Translation: Projects/Products*, Riga, Latvia, May 30–June 1 2016. Baltic Journal of Modern Computing.
- [63] J. T. Vogelstein, J. M. Conroy, V. Lyzinski, L. J. Podrazik, S. G. Kratzer, E. T. Harley, D. E. Fishkind, R. J. Vogelstein, and C. E. Priebe. Fast approximate quadratic programming for large (brain) graph matching. *PLoS One*, 2015.
- [64] J. T. Vogelstein and C. E. Priebe. Shuffled graph classification: Theory and connectome applications. *Journ. of Classification*, 32(1):3–20, 2015.
- [65] Haoyu Wang, Yihong Wu, Jiaming Xu, and Israel Yolou. Random graph matching in geometric models: the case of complete graphs. In *Conference on Learning Theory*, pages 3441–3488. PMLR, 2022.
- [66] S. Wang, J. Arroyo, J. T. Vogelstein, and C. E. Priebe. Joint embedding of graphs. *IEEE Transactions on Pattern Analysis and Machine Intelligence*, 2019.
- [67] S. Wasserman and K. Faust. *Social network analysis: Methods and applications*. Cambridge university press, 1994.

- [68] Y. Wu, J. Xu, and S. H. Yu. Settling the sharp reconstruction thresholds of random graph matching. *IEEE Trans. Info. Theory*, 68(8), 2022.
- [69] J. Yan, X. Yin, W. Lin, C. Deng, H. Zha, and X. Yang. A short survey of recent advances in graph matching. In *Proc. of the 2016 ACM on Int. Conf. on Multimedia Retrieval*, pages 167–174. ACM, 2016.
- [70] S. Young and E. Scheinerman. Random dot product graph models for social networks. In *Proceedings of the 5th international conference on algorithms and models for the web-graph*, pages 138–149, 2007.
- [71] Mingao Yuan and Qian Wen. A practical two-sample test for weighted random graphs. *Journal of Applied Statistics*, 50(3):495–511, 2023.
- [72] A. Zhang and D. Xia. Tensor svd: Statistical and computational limits. *IEEE Transactions on Information Theory*, 64(11):7311–7338, 2018.
- [73] Anru Zhang. Cross: Efficient low-rank tensor completion. *The Annals of Statistics*, 47(2):936–964, 2019.
- [74] Y. Zhang. Consistent polynomial-time unseeded graph matching for lipschitz graphons. *arXiv preprint arXiv:1807.11027*, 2018.
- [75] Y. Zhang. Unseeded low-rank graph matching by transform-based unsupervised point registration. *arXiv preprint arXiv:1807.04680*, 2018.
- [76] R. Zheng and M. Tang. Limit results for distributed estimation of invariant subspaces in multiple networks inference and pca. *arXiv preprint arXiv:2206.04306*, 2022.
- [77] M. Zhu and A. Ghodsi. Automatic dimensionality selection from the scree plot via the use of profile likelihood. *Computational Statistics & Data Analysis*, 51(2):918–930, 2006.
- [78] Xiaohan Zou. A survey on application of knowledge graph. In *Journal of Physics: Conference Series*, volume 1487, page 012016. IOP Publishing, 2020.

## A Proofs of main results

Herein we collect the proofs of the main results in this work. Below, we shall use the following notation. For a matrix  $\mathbf{M} \in \mathbb{R}^{n \times m}$  ( $n > m$ ), we denote the ordered singular values of  $\mathbf{M}$  via

$$\sigma_1(\mathbf{M}) \geq \sigma_2(\mathbf{M}) \geq \cdots \geq \sigma_m(\mathbf{M}).$$

For a square matrix  $\mathbf{M}$  with real spectrum, we will similarly use  $(\lambda_i(\mathbf{M}))_{i=1}^n$  to denote the ordered spectrum of  $\mathbf{M}$ .

Throughout, we will make use of the following Lemmas

**Lemma A.1** (Observation 2 in [32]). *Let  $F$  be a distribution on  $\mathbb{R}^d$  satisfying the  $\delta$ -inner product property, and let the  $n$ -rows of  $\tilde{\mathbf{X}}$  be i.i.d.  $F$  and let  $\mathbf{Y}$  independently distributed according to  $F$ . With probability at least  $1 - d^2/n^2$ , it holds that for all  $i \in [d]$ ,*

$$|\lambda_i(\tilde{\mathbf{X}}\tilde{\mathbf{X}}^T) - n\lambda_i(\mathbb{E}(\mathbf{Y}\mathbf{Y}^T))| \leq 2d\sqrt{n \log n}.$$

Lemma A.1, combined with assumption [ii]. on  $F$  then provides that there exist constants  $C_1 < C_2$  (only depending on  $F$ ) such that for  $n$  sufficiently large (i.e., for all  $n \geq n_0$  some  $n_0$  depending only on  $F$ )

$$C_1\sqrt{n} \leq \sigma_d(\tilde{\mathbf{X}}) \leq \sigma_1(\tilde{\mathbf{X}}) \leq C_2\sqrt{n} \quad (12)$$

holds with probability at least  $1 - d^2/n^2$ .

### A.1 Proof of Lemma 2.1

As in [34], we begin with (a slight extension of) Theorem 5.3.1 in [25]. We state the adapted version here (with our modification) as in [34].

Note that the error term in Eq. 14 is presented in non-asymptotic form here (which requires the slight proof modification provided below).

**Theorem A.1.** *Let  $\mathbf{W}$  be as in Lemma 1.1. Suppose that  $w_{\sigma^{(i)}(v)}, \hat{w}_{\sigma^{(i)}(v)} \in \mathbb{R}^d$  and  $r_{\sigma^{(i)}(v)}, \hat{r}_{\sigma^{(i)}(v)} \in \mathbb{R}^s$  satisfy*

$$\begin{aligned} \|\tilde{\mathbf{X}}\mathbf{W}w_{\sigma^{(i)}(v)} - \vec{b}_v^{(i)}\| &= \min_w \|\tilde{\mathbf{X}}\mathbf{W}w - \vec{b}_v^{(i)}\|, \quad r_{\sigma^{(i)}(v)} = \vec{b}_v^{(i)} - \tilde{\mathbf{X}}\mathbf{W}w_{\sigma^{(i)}(v)} \\ \|\hat{\mathbf{X}}_M^{(i)}\hat{w}_{\sigma^{(i)}(v)} - \vec{b}_v^{(i)}\| &= \min_w \|\hat{\mathbf{X}}_M^{(i)}w - \vec{b}_v^{(i)}\|, \quad \hat{r}_{\sigma^{(i)}(v)} = \vec{b}_v^{(i)} - \hat{\mathbf{X}}_M^{(i)}\hat{w}_{\sigma^{(i)}(v)}. \end{aligned}$$

*There exists constants  $D_0, D_1 > 0$  and  $s_0 \in \mathbb{Z}^+$  (all depending only on  $F$  and  $m$ ) such that for all  $s \geq s_0$ , we have that the following holds with probability at least  $1 - D_0/s^2$ :*

*i. We have that*

$$\|\hat{\mathbf{X}}_M^{(i)} - \tilde{\mathbf{X}}\mathbf{W}\| \leq \sigma_d(\tilde{\mathbf{X}}) \quad (13)$$

ii.  $\vec{b}_v^{(i)}$ ,  $w_{\sigma^{(i)}(v)}$  are all non-zero (note that to apply Eq. 5.3.11 from [25], we need not have  $r_{\sigma^{(i)}(v)} \neq 0$  as assumed in [34]);

iii.  $\tilde{\mathbf{X}}\mathbf{W}$  is rank  $d$ ;

iv. Define  $\theta_{\sigma^{(i)}(v)} \in (0, \pi/2)$  via  $\sin(\theta_{\sigma^{(i)}(v)}) = \|r_{\sigma^{(i)}(v)}\|/\|\vec{b}_v^{(i)}\|$ . Letting

$$\nu_{\sigma^{(i)}(v)} = \frac{\|\tilde{\mathbf{X}}\mathbf{W}w_{\sigma^{(i)}(v)}\|}{\sigma_d(\tilde{\mathbf{X}}\mathbf{W})\|w_{\sigma^{(i)}(v)}\|},$$

we have (where  $\kappa_2(\cdot)$  is the usual condition number of a matrix)

$$\begin{aligned} & \frac{\|\hat{w}_{\sigma^{(i)}(v)} - w_{\sigma^{(i)}(v)}\|}{\|w_{\sigma^{(i)}(v)}\|} \\ & \leq \frac{\|\hat{\mathbf{X}}_M^{(i)} - \tilde{\mathbf{X}}\mathbf{W}\|}{\|\tilde{\mathbf{X}}\mathbf{W}\|} (1 + \nu_{\sigma^{(i)}(v)} \tan \theta_{\sigma^{(i)}(v)}) \kappa_2(\tilde{\mathbf{X}}\mathbf{W}) + D_1 \frac{dm \log(mn)^2}{n} \frac{\|\hat{\mathbf{X}}_M^{(i)} - \tilde{\mathbf{X}}\mathbf{W}\|^2}{\|\tilde{\mathbf{X}}\mathbf{W}\|^2 \|w_{\sigma^{(i)}(v)}\|} \end{aligned} \quad (14)$$

We adapt the proof given in [25] here to provide the non-asymptotic form for the error. This will be key to our subsequent application of the OOS result to multiple vertices simultaneously.

*Proof.* Condition on the events in Eq. 2 and Eq. 12, so that parts [i]. and [iii]. in the theorem holds immediately. Indeed, conditioning on the aforementioned events (where  $C > 0$  is the constant appearing in Lemma 1.1)

$$\|\hat{\mathbf{X}}_M^{(i)} - \tilde{\mathbf{X}}\mathbf{W}\|^2 \leq \|\hat{\mathbf{X}}_M^{(i)} - \tilde{\mathbf{X}}\mathbf{W}\|_F^2 \leq \sum_{j=1}^s \|(\hat{\mathbf{X}}_M^{(i)} - \tilde{\mathbf{X}}\mathbf{W})_j\|^2 \leq C^2 m \log(ms)^2 = o(\sqrt{s}).$$

For part [ii]., by the  $\delta$ -inner product property assumption, the probability  $\vec{b}_v^{(i)}$  is zero is easily bounded above via Hoeffding's inequality by an exponentially small probability for  $s$  sufficiently large (with threshold on  $s$  only depending on  $F$ ); indeed we have that if  $Y \sim \text{Binom}(s, \delta)$ , then

$$\mathbb{P}(\|\vec{b}_v^{(i)}\|^2 = 0) \leq \mathbb{P}(Y = 0) \leq e^{-2s\delta^2}.$$

From  $\vec{b}_v^{(i)}$  being nonzero, we have that  $w_{\sigma^{(i)}(v)}$  would be non-zero as well giving part [ii]. in the theorem.

For part [iv]., we will follow the proof of Eq. 5.3.11 in [25] closely. Let

$$\epsilon = \frac{\|\hat{\mathbf{X}}_M^{(i)} - \tilde{\mathbf{X}}\mathbf{W}\|}{\|\tilde{\mathbf{X}}\mathbf{W}\|}$$

and define

$$E = \frac{\hat{\mathbf{X}}_M^{(i)} - \tilde{\mathbf{X}}\mathbf{W}}{\epsilon}.$$



Theorem 2.5.2 in [25] provides that  $\text{rank}(\tilde{\mathbf{X}}\mathbf{W} + t\mathbf{E}) = d$  for all  $t \in [0, \epsilon]$ . The solution  $x(t)$  to

$$(\tilde{\mathbf{X}}\mathbf{W} + t\mathbf{E})^T(\tilde{\mathbf{X}}\mathbf{W} + t\mathbf{E})x(t) = (\tilde{\mathbf{X}}\mathbf{W} + t\mathbf{E})^T\vec{b}_v^{(i)} \quad (15)$$

is continuously differentiable for all  $t \in [0, \epsilon]$ , and note that  $x(0) = w_{\sigma^{(i)}(v)}$ ,  $x(\epsilon) = \hat{w}_{\sigma^{(i)}(v)}$ . Differentiating Eq. 15 above, we arrive at the following

$$x(t) = \left( (\tilde{\mathbf{X}}\mathbf{W} + t\mathbf{E})^T(\tilde{\mathbf{X}}\mathbf{W} + t\mathbf{E}) \right)^{-1} (\tilde{\mathbf{X}}\mathbf{W} + t\mathbf{E})^T\vec{b}_v^{(i)} \quad (16)$$

$$\dot{x}(t) = \left( (\tilde{\mathbf{X}}\mathbf{W} + t\mathbf{E})^T(\tilde{\mathbf{X}}\mathbf{W} + t\mathbf{E}) \right)^{-1} \left( \mathbf{E}^T\vec{b}_v^{(i)} - ((\tilde{\mathbf{X}}\mathbf{W})^T\mathbf{E} + \mathbf{E}^T\tilde{\mathbf{X}}\mathbf{W} + 2t\mathbf{E}^T\mathbf{E})x(t) \right) \quad (17)$$

$$\ddot{x}(t) = \left( (\tilde{\mathbf{X}}\mathbf{W} + t\mathbf{E})^T(\tilde{\mathbf{X}}\mathbf{W} + t\mathbf{E}) \right)^{-1} \left( -2\mathbf{E}^T\mathbf{E}x(t) - 2((\tilde{\mathbf{X}}\mathbf{W})^T\mathbf{E} + \mathbf{E}^T\tilde{\mathbf{X}}\mathbf{W} + 2t\mathbf{E}^T\mathbf{E})\dot{x}(t) \right) \quad (18)$$

Note next that

$$\begin{aligned} \left\| \left( (\tilde{\mathbf{X}}\mathbf{W} + t\mathbf{E})^T(\tilde{\mathbf{X}}\mathbf{W} + t\mathbf{E}) \right)^{-1} \right\| &= (\sigma_d(\tilde{\mathbf{X}}\mathbf{W} + t\mathbf{E}))^{-2} \\ &\leq (\sigma_d(\tilde{\mathbf{X}}) - t\sigma_1(\mathbf{E}))^{-2} \\ &\leq \left( C_1\sqrt{s} - \frac{t}{\epsilon} \|\hat{\mathbf{X}}_M^{(i)} - \tilde{\mathbf{X}}\mathbf{W}\| \right)^{-2} \\ &\leq (C_1\sqrt{s} - Cm^{1/2}\log(ms))^{-2} \end{aligned}$$

where in the last line we applied Eq. 2. For  $s$  sufficiently large (bigger than a threshold  $s'_0$  depending on  $F$  and  $m$ ), we then have that there exists a constant  $C_3$  (depending on only  $F$  and  $m$ ) such that

$$\|[(\tilde{\mathbf{X}}\mathbf{W} + t\mathbf{E})^T(\tilde{\mathbf{X}}\mathbf{W} + t\mathbf{E})]^{-1}\| \leq C_3/s \quad (19)$$

Applying this to Eq. 16–18, we have that for  $s$  sufficiently large (bigger than a threshold  $s''_0$  depending on  $F$  and  $m$ ) there exists constants  $C_4, C_5, C_6 > 0$  (independent of  $\vec{b}_v^{(i)}$ ) such that for any  $t$ ,

$$\begin{aligned} \|x(t)\| &\leq C_3/s \cdot (C_2\sqrt{s} + Cm^{1/2}\log(ms))\sqrt{s} \leq C_4 \\ \|\dot{x}(t)\| &\leq C_3/s \cdot (C(m s)^{1/2}\log(ms) + 2C_4C_2C(ms)^{1/2}\log(ms) + 2C_4C^2m\log(ms)^2) \\ &\leq C_5 \frac{m^{1/2}\log(ms)}{\sqrt{s}} \\ \|\ddot{x}(t)\| &= C_3/s \cdot \left( 2C_4C^2m\log(ms)^2 + 4C_5C_2Cm\log(ms)^2 + 2C_5C^2 \frac{m^{3/2}\log(ms)^3}{\sqrt{s}} \right) \\ &\leq C_6 \frac{m\log(ms)^2}{s} \end{aligned}$$

A Taylor expansion then yields

$$\hat{w}_{\sigma^{(i)}(v)} = w_{\sigma^{(i)}(v)} + \epsilon \dot{x}(0) + \epsilon^2 R_2$$

where the remainder term  $R_2$  satisfies

$$\|R_2\| \leq C_6 \frac{dm \log(ms)^2}{2s}$$

from the above bound on  $\|\ddot{x}(t)\|$  (which we note is uniform on  $t \in [0, \epsilon]$ ).

This yields that

$$\frac{\|\hat{w}_{\sigma^{(i)}(v)} - w_{\sigma^{(i)}(v)}\|}{\|w_{\sigma^{(i)}(v)}\|} = \epsilon \frac{\|\dot{x}(0)\|}{\|w_{\sigma^{(i)}(v)}\|} + \epsilon^2 \frac{\|R_2\|}{\|w_{\sigma^{(i)}(v)}\|}. \quad (20)$$

Now

$$\begin{aligned} \dot{x}(0) &= \left( (\tilde{\mathbf{X}}\mathbf{W})^T (\tilde{\mathbf{X}}\mathbf{W}) \right)^{-1} \left( \mathbf{E}^T \vec{b}_v^{(i)} - ((\tilde{\mathbf{X}}\mathbf{W})^T \mathbf{E} + \mathbf{E}^T \tilde{\mathbf{X}}\mathbf{W}) w_{\sigma^{(i)}(v)} \right) \\ &= \left( (\tilde{\mathbf{X}}\mathbf{W})^T (\tilde{\mathbf{X}}\mathbf{W}) \right)^{-1} \mathbf{E}^T r_{\sigma^{(i)}(v)} - \left( (\tilde{\mathbf{X}}\mathbf{W})^T (\tilde{\mathbf{X}}\mathbf{W}) \right)^{-1} (\tilde{\mathbf{X}}\mathbf{W})^T \mathbf{E} w_{\sigma^{(i)}(v)} \end{aligned}$$

We then have that

$$\begin{aligned} \|\dot{x}(0)\| &\leq \left\| \left( (\tilde{\mathbf{X}}\mathbf{W})^T (\tilde{\mathbf{X}}\mathbf{W}) \right)^{-1} \mathbf{E}^T r_{\sigma^{(i)}(v)} \right\| + \left\| \left( (\tilde{\mathbf{X}}\mathbf{W})^T (\tilde{\mathbf{X}}\mathbf{W}) \right)^{-1} (\tilde{\mathbf{X}}\mathbf{W})^T \mathbf{E} w_{\sigma^{(i)}(v)} \right\| \\ &\leq \frac{\|\tilde{\mathbf{X}}\| \cdot \|r_{\sigma^{(i)}(v)}\|}{\sigma_d(\tilde{\mathbf{X}})^2} + \frac{\|\tilde{\mathbf{X}}\| \cdot \|w_{\sigma^{(i)}(v)}\|}{\sigma_d(\tilde{\mathbf{X}})} \end{aligned}$$

Plugging this into Eq. 20 yields that

$$\frac{\|\hat{w}_{\sigma^{(i)}(v)} - w_{\sigma^{(i)}(v)}\|}{\|w_{\sigma^{(i)}(v)}\|} \leq \epsilon \left( \frac{\|\tilde{\mathbf{X}}\| \cdot \|r_{\sigma^{(i)}(v)}\|}{\sigma_d(\tilde{\mathbf{X}})^2 \|w_{\sigma^{(i)}(v)}\|} + \frac{\|\tilde{\mathbf{X}}\|}{\sigma_d(\tilde{\mathbf{X}})} \right) + \epsilon^2 \frac{\|R_2\|}{\|w_{\sigma^{(i)}(v)}\|}.$$

Now  $\cos(\theta_{\sigma^{(i)}(v)}) = \|\tilde{\mathbf{X}}\mathbf{W} w_{\sigma^{(i)}(v)}\| / \|\vec{b}_v^{(i)}\|$  and  $\tan(\theta_{\sigma^{(i)}(v)}) = \|r_{\sigma^{(i)}(v)}\| / \|\tilde{\mathbf{X}}\mathbf{W} w_{\sigma^{(i)}(v)}\|$ . Plugging this into the above yields the desired result. Again, we note this proof closely followed the analogous proof of Theorem 5.3.1 in [25] (noting that here  $f = 0$  in the notation of [25]).  $\square$

We next turn our attention to proving Lemma 2.1; note we closely follow the analogous proof of Theorem 7 in [34].

*Proof.* Applying Lemma 25 in [34] yields that there exists a constant  $\gamma \in (0, 1)$  (depending only on  $F$ ; the key being the  $\delta$ -inner product property) such that with probability at least  $1 - D_2 n^{-2}$  ( $D_2$  here depending only on  $F$ ),

$$\cos \theta_{\sigma^{(i)}(v)} \geq \gamma. \quad (21)$$

Next, following the proof of Theorem 7 in [34], we define  $\vec{r} = \vec{b}_v^{(i)} - \tilde{\mathbf{X}}\mathbf{W}(\mathbf{W}^T X_v)$ , and we note that  $\|r_{\sigma^{(i)}(v)}\| \leq \|\vec{r}\|$ . We then have that

$$\|\vec{r}^T \tilde{\mathbf{X}}\mathbf{W}\|^2 = \|\vec{r}^T \tilde{\mathbf{X}}\|^2 = \sum_{k=1}^d \left( \sum_{j=1}^n ((\vec{b}_v^{(i)})_j - \tilde{\mathbf{X}}_j^T X_v) \tilde{\mathbf{X}}_{jk} \right)^2$$

For each  $k$ , conditioning on  $\tilde{\mathbf{X}}$  and  $X_v$  we note that the sum (over  $j$ ) is the sum of  $s$  mean 0 independent random variables uniformly bounded in  $[-1, 1]$  (bounded here uniformly for all  $\vec{b}_v^{(i)}$ ) and that Hoeffding's inequality yields

$$\begin{aligned} & \mathbb{P} \left( \left| \sum_{j=1}^s ((\vec{b}_v^{(i)})_j - \tilde{\mathbf{X}}_j^T X_v) \tilde{\mathbf{X}}_{jk} \right| \geq 20\sqrt{s \log s} \right) \\ &= \mathbb{E} \left[ \mathbb{P} \left( \left| \sum_{j=1}^s ((\vec{b}_v^{(i)})_j - \tilde{\mathbf{X}}_j^T X_v) \tilde{\mathbf{X}}_{jk} \right| \geq 20\sqrt{s \log s} \mid \tilde{\mathbf{X}}, X_v \right) \right] \\ &\leq \exp(-5 \log^2 s) \leq s^{-5} \end{aligned}$$

Taking a union over the  $d$  values of  $k$ , we have that

$$\mathbb{P}(\|\vec{r}^T \tilde{\mathbf{X}}\|^2 \leq 400ds \log s) \geq 1 - ds^{-5}. \quad (22)$$

Next note that conditioning on the events in Eq. 2, Eq. 12, Eq. 21, and Eq. 22 we have that  $\nu_{\sigma^{(i)}(v)} \leq \frac{C_2}{C_1}$ , and  $\kappa_2(\tilde{\mathbf{X}}\mathbf{W}) \leq \frac{C_2}{C_1}$  as well. We then have

$$\begin{aligned} & \frac{\|\hat{w}_{\sigma^{(i)}(v)} - w_{\sigma^{(i)}(v)}\|}{\|w_{\sigma^{(i)}(v)}\|} \\ &\leq \frac{\|\hat{\mathbf{X}}_M^{(i)} - \tilde{\mathbf{X}}\mathbf{W}\|}{\|\tilde{\mathbf{X}}\mathbf{W}\|} (1 + \nu_{\sigma^{(i)}(v)} \tan \theta_{\sigma^{(i)}(v)}) \kappa_2(\tilde{\mathbf{X}}\mathbf{W}) + D_1 \frac{dm \log(ms)^2}{s} \frac{\|\hat{\mathbf{X}}_M^{(i)} - \tilde{\mathbf{X}}\mathbf{W}\|^2}{\|\tilde{\mathbf{X}}\mathbf{W}\|^2 \|w_{\sigma^{(i)}(v)}\|} \\ &\leq \frac{Cm^{1/2} \log(ms)}{C_1 s^{1/2}} \left( 1 + \frac{C_2}{C_1 \gamma} \right) \frac{C_2}{C_1} + \frac{D_1 C^2 dm^2 \log^4(ms)}{C_1^2 s^2 \|w_{\sigma^{(i)}(v)}\|} \end{aligned}$$

implying that

$$\|\hat{w}_{\sigma^{(i)}(v)} - w_{\sigma^{(i)}(v)}\| \leq C_4 \frac{Cm^{1/2} \log(ms)}{C_1 s^{1/2}} \left( 1 + \frac{C_2}{C_1 \gamma} \right) \frac{C_2}{C_1} + \frac{D_1 C^2 dm^2 \log^4(ms)}{C_1^2 s^2}. \quad (23)$$

Following the proof of Lemma 27 in [34] Noting that

$$\|\vec{r}\| \geq \|\vec{b}_v^{(i)} - \tilde{\mathbf{X}}\mathbf{W}w_{\sigma^{(i)}(v)}\| = \|\tilde{\mathbf{X}}\mathbf{W}\mathbf{W}^T X_v + \vec{r} - \tilde{\mathbf{X}}\mathbf{W}w_{\sigma^{(i)}(v)}\|$$

we then have that

$$\sigma_d^2(\tilde{\mathbf{X}}) \|w_{\sigma^{(i)}(v)} - \mathbf{W}^T X_v\|^2 \leq \|\tilde{\mathbf{X}}\mathbf{W}(w_{\sigma^{(i)}(v)} - \mathbf{W}^T X_v)\|^2 \leq 2(\vec{r})^T \tilde{\mathbf{X}}\mathbf{W}(w_{\sigma^{(i)}(v)} - \mathbf{W}^T X_v)$$

from which we have (via Cauchy-Schwartz)

$$\|w_{\sigma(i)(v)} - \mathbf{W}^T X_v\|^2 \leq \frac{2(\vec{r})^T \tilde{\mathbf{X}} \mathbf{W} (w_{\sigma(i)(v)} - \mathbf{W}^T X_v)}{C_1^2 s} \leq \frac{2\|(\vec{r})^T \tilde{\mathbf{X}}\| \cdot \|w_{\sigma(i)(v)} - \mathbf{W}^T X_v\|}{C_1^2 s}$$

We then have (assuming  $\|w_{\sigma(i)(v)} - \mathbf{W}^T X_v\| > 0$ , as equaling 0 would immediately provide the bound in Eq. 24),

$$\|w_{\sigma(i)(v)} - \mathbf{W}^T X_v\| \leq 2 \frac{\|(\vec{r})^T \tilde{\mathbf{X}}\|}{C_1^2 s} \leq \frac{20\sqrt{d \log s}}{C_1^2 \sqrt{s}} \quad (24)$$

Combining Eq. 24 and Eq. 23 and the boundedness of  $x(t)$  (and hence of  $w_{\sigma(i)(v)}$ ) yields the desired result.  $\square$

## B Additional figures and simulations

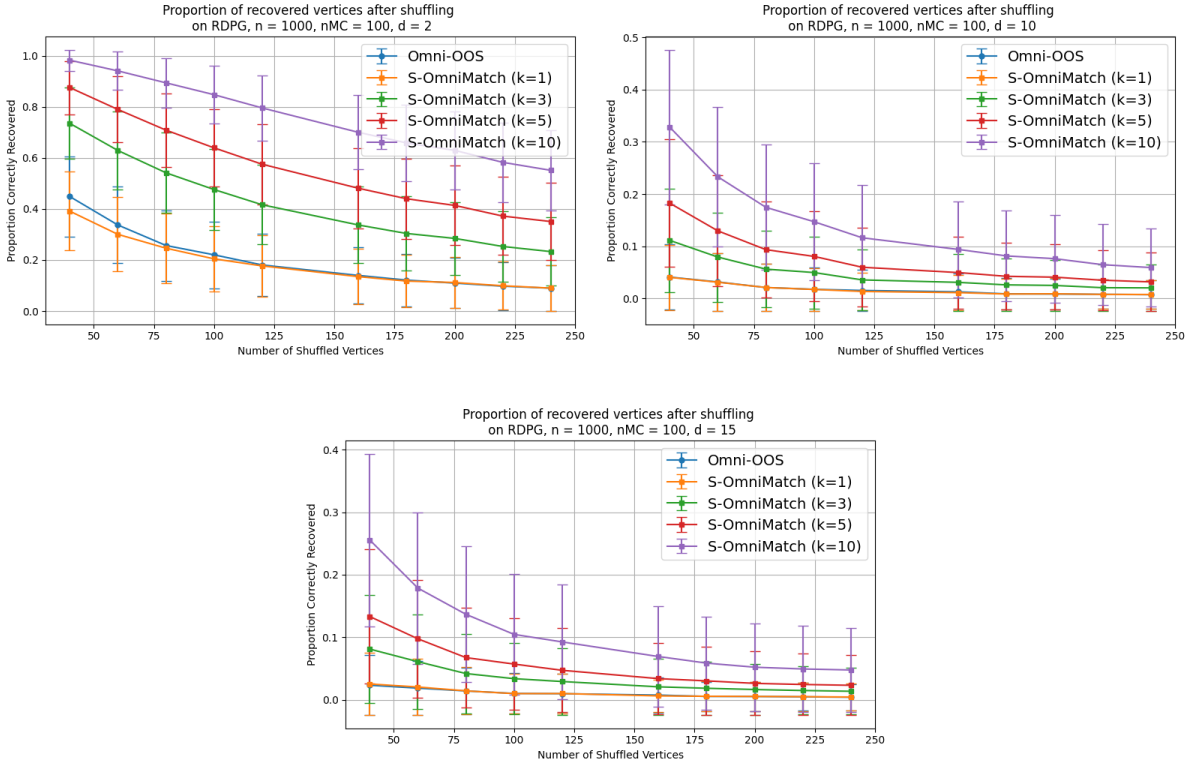


Figure 8: The proportion of correctly unshuffled vertices for OmniMatch and S-OmniMatch using the  $k = 1, 3, 5, 10$  nearest neighbors for two- (top-left), ten- (top-right) and fifteen-dimensional RDPG with 1000 vertices. Results are averaged over  $nMC = 100$  simulations.

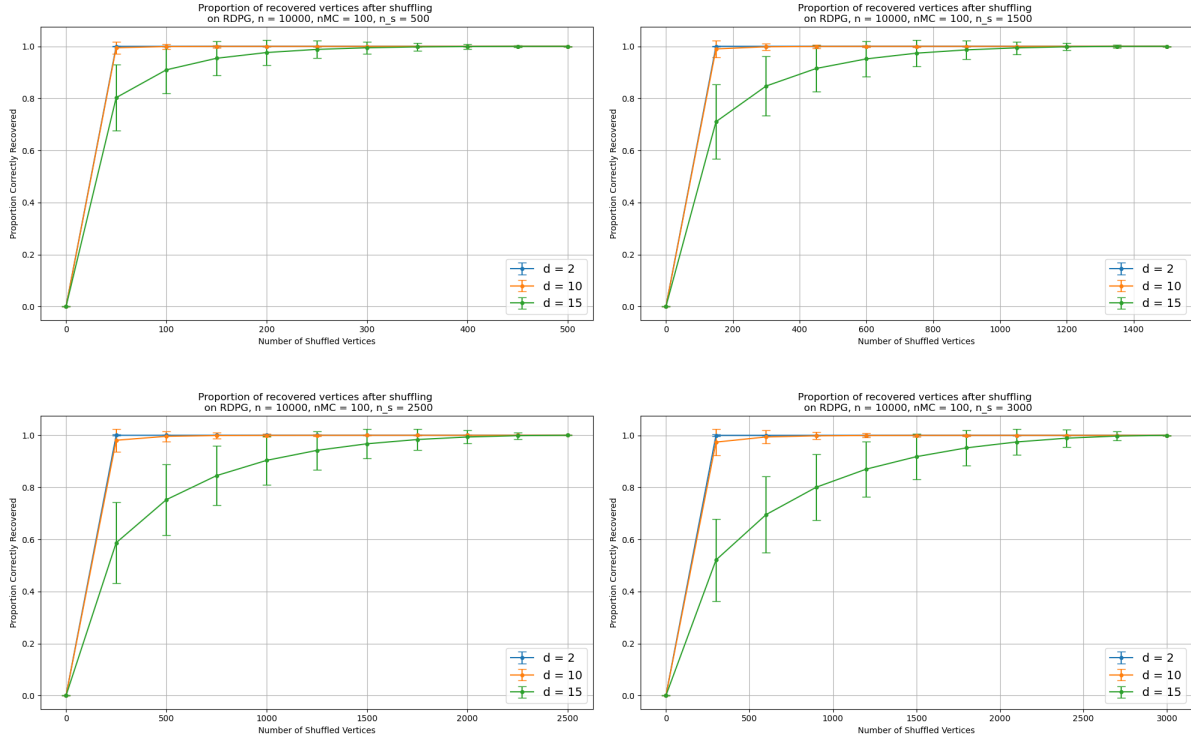


Figure 9: Precision plots for the proportion of correctly unshuffled vertices with  $n_s = 500, 1500, 2500, 3000$  shuffled vertices, where the number of neighbors used in S-OmniMatch ranges from 1 to  $n_s$ . Results are averaged over  $nMC = 100$  simulations for embeddings of dimensions two, ten, and fifteen of the RDPG with 10,000 vertices.

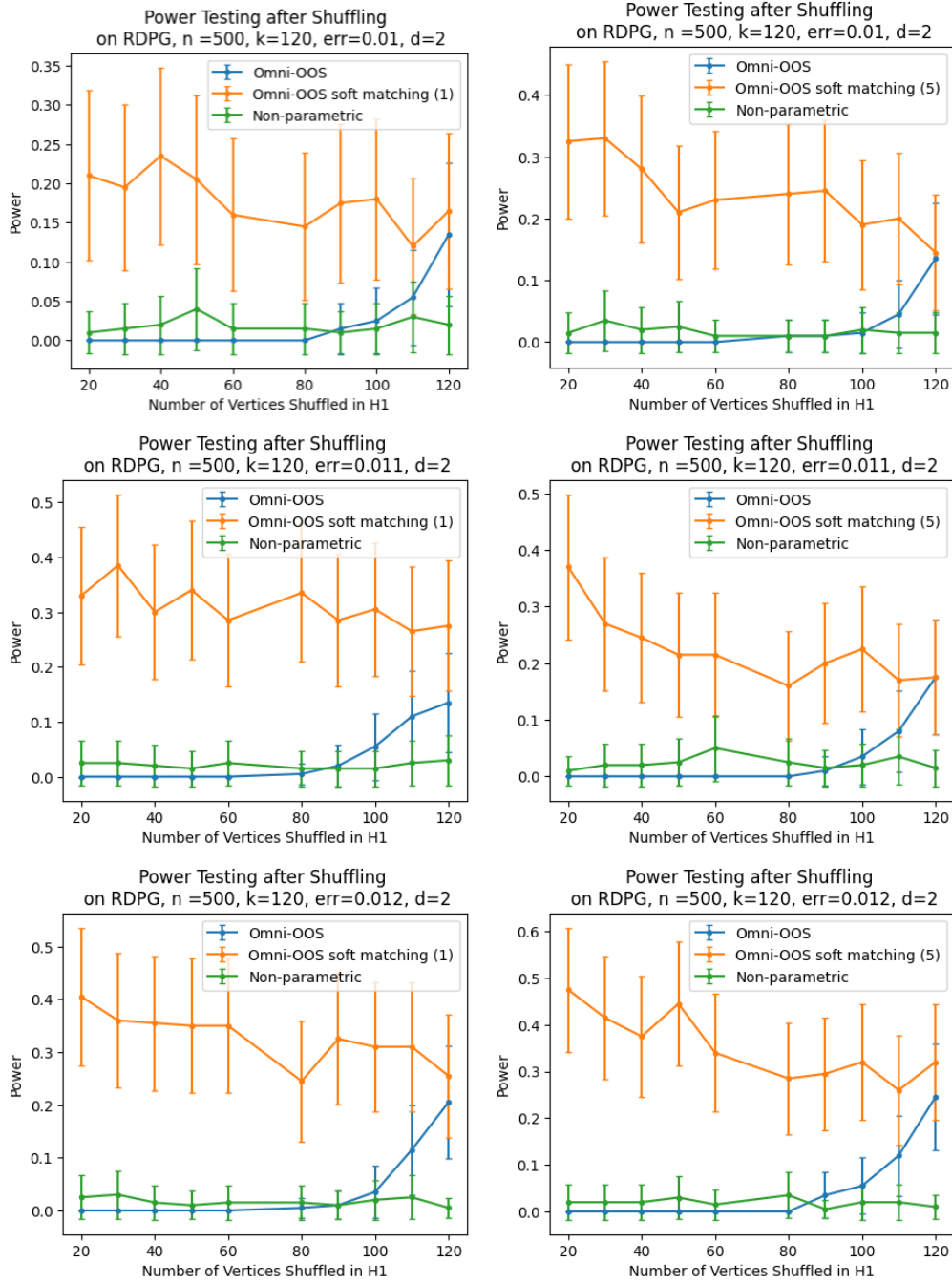


Figure 10: Statistical power for two-sample graph hypothesis testing under node shuffling. Each panel displays results from experiments on pairs of graphs with  $n = 500$  nodes. For each pair, one graph is fixed while the other has noise with  $error \in 0.01, 0.011, 0.012$  added to the lated positions. All embeddings are performed in dimension 2. The three panels on the left compare the empirical testing power of **OmniMatch**, **S-OmniMatch** using 1 nearest neighbor, and a non-parametric test. The three panels on the right include **S-OmniMatch** with 5 nearest neighbors.